



Tallinn University of Technology

MEHHATROONIKA INSTITUUT

MHK70LT

.....

**DEVICE FOR SPATIAL DISTRIBUTION MEASUREMENT OF
PARTICLES IN A BEAM OF PROTONS**

Prootonkiire osakeste ruumilist jaotust mõõtev seade

Author
master of science
Lazarev Aleksandr

Tallinn 2015

MASTER'S THESIS SHEET OF TASK'S

Year 2015 semester 2

Student: Aleksandr Lazarev 150701MV

Curricula: Mechanics

Speciality: Mechatronics

Supervisor: Research Scientist, Mairo Hiiemaa

MASTER'S THESIS TOPIC:

Device for Spatial Distribution Measurement of Particles in a Beam of Protons

Thesis tasks to be completed and the timetable:

Nr	Description of tasks	Timetable
1.	Decide on the goal of the thesis	07.02.2015
2.	Design of the prototype of the device	20.03.2015
3.	Build of the prototype and testing it	06.04.2015
4.	Testing prototype in operational environment, experimental works at the enterprise	16.04.2015
5.	Release version of device, written part of the work finished	09.05.2015

Solved engineering and economic problems: Analyzing of the task given from enterprise, choosing sensors for the project, designing the construction, characteristics of main project components, requirement for the construction, development of the control algorithms (control of the stepper motor system), development of the signal processing algorithms.

Additional comments and requirements:

.....

Language: English

Application is filed not later than 12.05.2015

Deadline for submitting the theses 22.05.2015

Student /signature/ date

Supervisor /signature/ date.....

Confidentiality requirements and other conditions of the company are formulated as a company official signed letter

Eessõna

Selle lõputööga seotud töö teostati PNPI-s (Saint-Petersburg Nuclear Physics Institute). Projekt pakuti välja PNPI prootonteraapia töörühma direktori Dzhan Karlini poolt. Lõputöö eesmärgiks oli välja töötada seade, mis on võimeline mõõtma osakeste ruumilist jaotust prootonkiires.

Prooton teraapia on meditsiiniline toiming peaaegu mitesuguste haiguste raviks kirurgilise sekkumiseta. Teraapia on väga heade tulemustega ja tõhus. Ravi tulemuslik lõpetamine on fikseeritud 85% juhtudest. Seni pole fikseeritud ühtegi kaebust prooton teraapia kõrvalnähtude kohta.

Prooton teraapia protseduuride tõhusus sõltub väga suuresti selle täpsusest. Kuna meditsiiniline töögrupp seadis prootonkiire pofilile prooton raviks spetsiifilised parameetrid, on oluline taastada need täpsed parameetrid iga protseduuri tsükliks. Seetõttu kasutatakse selle ülesande juures väga täpseid tööriistu ja seadmeid.

Mitmeid seadmeid kasutatakse selleks, et luua õiged prootonkiire parameetrid teekonnal patsiendi pähe. Minu ülesanne selles töös oli seadme väljatöötamine, mis võimaldab mõõta prootonkiire parameetreid vahetult kiire lõplikus kiirituse piirkonnas.

Abstract

The work of this thesis was performed for Saint-Petersburg Nuclear Physics Institute (PNPI). The project was proposed by director of proton therapy group of PNPI Dzhan Karlin. The purpose of the thesis was to develop device that is able to measure spatial distribution of particles in a beam.

Proton therapy is medical procedure for treating various head brain diseases such as arteriovenous malformations and pituitary adenoma without resort to surgery methods. Therapy shows very good results and high effectiveness. Remission without repeated proton therapy is fixed in 85% of cases. No even single complain from patients about side effects of proton therapy treatment were fixed.

Effectiveness of proton therapy procedure is very dependant on its accuracy. Since medical group set specific parameters of beam profile as optimal for proton therapy procedure it is necessary to reconstruct those exact parameters for each procedure cycle. So very precise tools and devices those are able to perform this task have to be used.

Several devices are used to form correct beam parameters on its way to patients head. My part in this work was to design device that are able to measure beam parameters on the final stage of beam forming in immediate area of irradiation.

Device had to be designed in accordance with provided by enterprise technical task (translated version is attached in appendix).

Content

Proton therapy method	8
Description of the proton therapy method, used tools and devices	8
Description of the proton beam measurement device	12
Technical task analysis	14
Detector part	15
Review of existing detectors.....	15
Scheme of sample and store	27
Analog switch controlling microchip	29
Sample and store possible modifications.....	34
Mechanical part	35
Control part.....	37
Algorithm of reconstruction of beam spatial distribution	37
Interpolation algorithm	45
Working cycle algorithm	47
Interface of PC program	49
Components used.....	50
Arduino Uno	51
Arduino motor shield v1.2.....	57
L293D motor driver.....	59
PCB with switches and memory multiplexor	61
Step down voltage convertor LM2596	62
Conclusions	64
Appendix	69
PCB.....	69
Photo.....	70
Schemes	71
Technical task.....	76

Introduction

Since the guess of Maria and Pierre Curie in early 1901 to use radioactivity discovered 6 years before in medical purpose for treating tumors, radiotherapy becomes widely used nowadays. High energy of elementary particles is commonly used now to destroy or damage diseased cells. Destructive power of such energy that Curie couple experienced on themselves has to be correctly controlled and measured so it become healing energy. Balance between damage that unavoidably caused as to diseased tissue as to healthy one by radiotherapy procedure is still main problem of this range.

Radiotherapy is widely know in domain of cancer treating. In that case usually used particles in the range of energy 70-250 MeV and negative effect on healthy cells caused by energy of elementary particles is reduced by using depth dose distribution. Effect when the particles loses their energy with a splash at a certain depth in human body is known as Bragg peak. Although in this method tissue located at the further depth doesn't get a dose, elementary particles with such velocity has a quite large lateral scattering that produces a dose halo in the patients body. Usage of heavy particles and particles with higher velocity reduce the lateral scattering and dose fields in this case can have more sharp edges.

Idea of using particles with more higher energy was put into action at Saint-Petersburg Nuclear Physics Institute (PNPI) where proton ray synchrocyclotron previously used only in science purpose became used at 1975 in the field of radio neurosurgery. This synchrocyclotron accelerates particles up to the energy of 1 GeV. Particles with such high velocity cannot be used in the Bragg peak method, cause of its long range (for example 3.2m in water [4]). But the advantage is a stable beam profile with very sharp edges and rather low scattering caused by the 1 GeV proton beam on its way trough the patient's body. High energy beam has a small cross section size of about 6 on 6 mm on half dose and in combination of rotation technique it can be used for creation a necessary high dose concentration in a certain depth of irradiated object with low concentration at the object surface. Accordingly to the researches guided at the PNPI the ratio of the dose in the centre to the dose at the surface is 200:1 [3]. Since the 1975 the course of proton therapy was given to about 1500 patients, and no even single appearance of side effects was registered [3]. Method of proton stereotactic therapy at the PNPI shows a high effectiveness at the various head brain diseases such as arteriovenous malformations and pituitary adenoma usually treated as inoperable by traditional neurosurgery. Remission without repeated proton therapy is fixed in 85% of cases and complete recovery from mentioned deceases

was obtained in 55% of cases [3]. Efficiency of the method beside the other factors is highly dependable on the accuracy of beam forming and measuring.

A lot of different tools and devices are used at PNPI center of proton therapy to control the dose concentration in the irradiation object and to measure a beam energy and spatial distribution of proton on their way to the object of irradiation. There are several magnetic corrector and collimators used to control the beam characteristics on its way to recurve it from main tract to the medical department and to control its size. Special rotation device also controls the dose concentration at the beam's final destination by rotation object of irradiation around two separate axis on the way of the beam. Proton beam also pass through lot of different devices those are able to measure and store its different parameters such as energy and spatial distribution. Although the parameters of the beam are quite stable on the whole way through the proton therapy room it is very important for the efficiency of procedure to control its characteristics in direct area of object of irradiation. Moreover it is very important to know the immediate form and spatial distribution of particles in beam cross section at those particular points.

Such device that can be placed at the immediate area of irradiation and is able to measure and store the full information of the beam profile was constructed and successfully tested by the engineers of PNPI. Several researches were made and papers were published using that prototype. This device approved possibility of using semiconductor detector for precise measuring of beam profile. Although the prototype is quite heavy, slow and its construction doesn't correlate with other used devices. So it was decided to design a new version of this device, light weighted, easy transportable, that can be easily attached to the existing devices, and has reworked algorithm of scanning that allows to make the procedure a lot more faster than it was. That task of designing such a device was suggested to me as work I can develop within a context of my master thesis. The technical task to this device provided to me by the director of proton therapy group of PNPI is attached to at the end of this paper, it has fluent description and main expected characteristics of device.

Proton therapy method

Before proceeding to direct subject of the task it is necessary for better understanding to describe procedure of proton therapy itself. Tools and devices those are used to measure and control beam parameters on its way to area of irradiation will be described in details in the next chapter.

Description of the proton therapy method, used tools and devices

Proton therapy room that can be seen at the figure below is equipped with lot of diagnostic tools and devices. Before arriving at the room of proton therapy beam travels a long way approximately 70m from synchrocyclotron. Along the whole length beam travels inside vacuum tube that protects beam from natural scattering as result of air friction and obstruction with other particles that can be generated in the ionization process. To recurve protons of the beam from main tract to medical department special magnetic lenses are used. Proton tract itself as vacuum tube and magnetic lenses can be seen a the right part of the photo. Behind it to the left is located rotation device with a medical table where patient can be placed. To this device attached X-ray apparatus that is able to rotate on fixed angles around medical table to shoot a object of irradiation (patient's head) in 2 orthogonal planes. At the wall opposite to proton ray tract there are marked point at which beam strikes. There are radiation absorbent and scintillation counter located at the edge of the beam that just signalize about beam arrival in the most simplest way.



Figure 1. Proton therapy room

The heart of the stereotactic proton therapy is rotation device with medical table that is called proton stereotactic therapy device (UPST). Cause beam is produced in range of about 70 meters away from the object of irradiation it cannot be rotated around the object by the reason of its constructional features, so the necessary dose concentration in the selected point can be achieved by the rotation of the object itself around that point. Construction of the proton stereotactic therapy device (figure 2) allow rotation of the medical table with a patient attached to it around ground plane in range of $\pm 40^\circ$ and rotation of the patient's head fixed in special device around axis passing through the patient's body in range of $\pm 36^\circ$. Procedure of irradiation takes about 10 minutes while stereotactic device executes slowly swinging rotations around 2 separate axis those do not cause any negative feelings to the patient but form a demand dose field in the center of rotation, that sufficiently high in comparison to those formed at the surface.



Figure 2. Proton stereotactic therapy device

A lot of different calibration tools are situated on the way of the beam to control its parameters. *Ionization chambers* gives information about energy of particles by measuring ionization energy of gas sealed in the chamber caused by the elementary particles passing through it. Construction of *proportional chamber* in common way allows to get information not only about energy but also about certain point where particles passed through the chamber. It also filled with the gas and has 2 orthogonal rows of ionization sensitive wires. Information about practical appearance taken from 2 orthogonal wires gives X and Y information about its position in the passed volume. But in our case when particles go through the detector as a beam time resolution of the chamber does not allow us to get information about each particular particle. Information taken in this way are projections of beam profile on two orthogonal planes. Unfortunately this information does not allow us to reconstruct a proper beam profile. Both proportional and ionization chambers (Figure 3) are used in pairs and are active at the whole time of procedure so any changes of energy or projection of beam profile can be instantly detected.

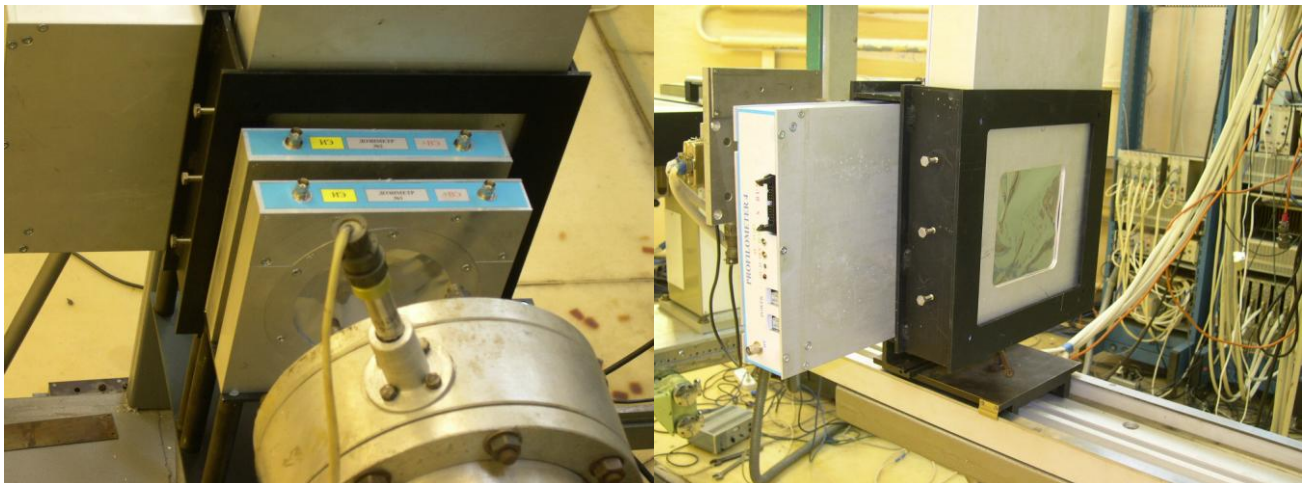


Figure 3. Pairs of ionization (left) and proportional chambers (right) are used to control parameters of proton beam

For setting correct parameters of medical procedure it is necessary to get information at the area of irradiation. X-ray machine is attached to the proton therapy is able to rotate in fixed angles around medical table. Image from the X-ray machine can be instantly displayed at the monitor located near medical table. It allows to take X-ray image of the patient's head in two orthogonal projections and detect the spatial location of diseased tissues. Usually proton therapy team just has to find on the image special markers in the patient's head those were implanted by medics previously. Markers injected under

the skin of patient's head are small metallic parts so could be easily seen at the screen. X-ray machine rotated in the horizontal position and the monitor can be seen at the photo below.



Figure 4. X-ray machine and monitor with instantly displayed image

After correct point have been found and loaded to the memory of computer that controls UPST a real profile of the beam at the area of irradiation has to be achieved. Information about size of the beam profile and point of maximal intensity are very important for successful results. Special calibration tool shown at the figure 5 is used to measure such parameters of the beam. Calibration tool can be attached to the UPST at the place where will be patient's head. Device has slots for particles sensitive photo paper, those situated symmetrically at both sides and has a fixture at centre for phantom head. The head phantom has separate ionization sensitive parts made of LiF. Phantom can be used to simulate human's head in the cycle proton therapy procedure to check how much dose concentration will take different areas of head. Two photo sensitive papers record get an image of beam profile at the entrance of head and at exit from it. This information cannot be achieved instantly and have to be analyzed after irradiation process has been stopped.

To get on-line information about beam profile a special device was designed.



Figure 5. Calibration tool with slot for photo paper and ionization sensitive phantom head

Description of the proton beam measurement device

Device that used at PNPI as proton beam profilometer was constructed about 10 years ago. It has ionization sensitive detector that perform line by line scanning of the whole area of beam cross section. Device is shown at the following figure

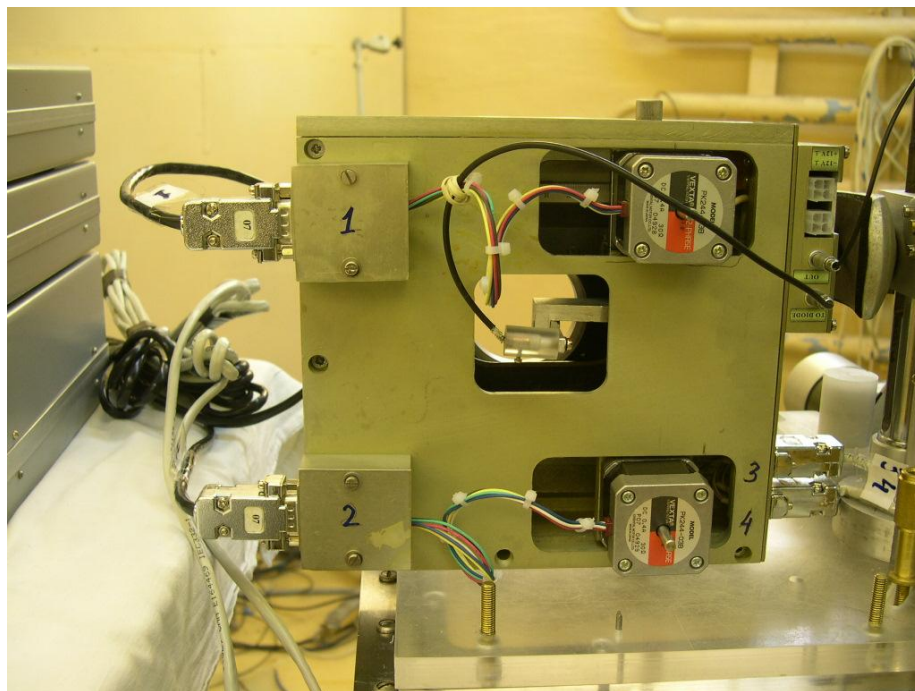


Figure 6. Proton beam profilometer

As detector part device has semi conductive sensor with size approximately 1mm. Workability of such type of sensor for demands of proton therapy was previously approved by several researches guided by proton therapy group at PNPI. Mechanical part in this device has 2 translational axis and uses 2 stepper motors. One of this axis connected to the other so single sensor is able to move in the whole area of beam cross section. Data achieved by the sensor goes directly to PC via COM port where whole image of cross section of the beam can be reconstructed.

Although usage of a single sensor as detector part has a lot of advantages working algorithm that perform all area scanning is sufficiently slow (about 15 minutes). Also as can be seen from the mentioned figure device is quite big, heavy and has no special fixtures those correlates with other used tools and devices. For example calibration tool has to be removed to allow enough place for this device. All of mentioned disadvantages has to be removed in the new design of this device. Requirements of the technical task will be considered in depth in the following chapter.

Technical task analysis

(Technical task is attached to this work at the appendix)

Main requirements to design of the device are listed in the following table.

Bounding box:	133mm 20mm 145mm
Analog channels:	8
Maximal movement range:	18mm
Time of full measurement cycle:	less than 1-2 mins
Dimension resolution:	0.15mm
Type of the semiconducting detector:	Si diode in SOD523 package, SOD123
Supply voltage:	+5V

Bounding box is mentioned to correspond to the slots, fixtures and size of the calibrated tool where device is planned to be set. Detection part of device have to be redesigned so instead of single sensor from 4 or 8 sensor per axis will be used. So the minimal number of analog channels expected from MCU is 8. Movement range has to be enough to allow sensor to go out of beam.

To perform this action is also necessary to attach a null position detector to each axis. Translation movements along axis have to provide minimal dimensional resolution of 0.1 mm. It is suggested to use semi conductive type sensor as sensitive unit in detector part, more specifically Si diode in SOD523 those were used in prototype and those sensitive characteristics were approved by experiments [1]. As soon as it is planed to use several sensitive units instead of 1 work algorithm have to be redesigned also. It is no more necessary to have 2 dependant transition movements of axis. Two sensitive parts can be moved separately scanning beam profile along each axis. Sensitive units unavoidably will suffer from damage caused by particles action and degrade, so detective part of device have to be easily replaceable and cheap enough. Cause each sensitive unit has different initial sensitivity and different speed of degradation in time caused by irradiation, it is also necessary to foresee an algorithm of auto calibration of axis.

Intensively from beam to beam is a bit different so averaging mechanism has to be carried out.

Detector part

Review of existing detectors

There are two main groups of elementary particle: counters and track Detectors of elementary particles are usually separated by its assignment in two groups: particle counters and track detectors. Counter is used for registration of particle passing through selected spatial domain and fixation its time. Track detectors allow to define particle trajectory.

As counters commonly are also treated detectors those are able not only registry the time of particle passing but also determine other characteristics of a particles such as energy, charge, mass, velocity and etc..

Main characteristics of part are:

Effectiveness - ratio of particles registered by detector to the full number of particles passed through the volume of detector.

Spatial resolution - accuracy of determination of particle position in space.

Time resolution - minimal length of time between two particles passed through the volume of detector so detector be able to determine those particles as two different.

Reset time - time that detector spend on saving information about previous particle and return to the state ready for registration of the next.

Lets take a close look at the counter type detectors. Many of the counters invented and used so far are ionization detectors. Ionization in this case is a process of dissipation of atoms of the material caused by high energy elementary particle passing through its volume.

Ionization chamber is closed volume, filled with gas, where cathode and anode are placed. For simplicity a chamber can be represented as a capacitor. Scheme can be seen at the following figure. By applying a voltage to electrodes in the volume of detector caused electrical field. When elementary particle causes ionization process in the matter of detector newly created charged ions flow under the influence of electrical field to the opposite electrodes. Current induced when ions reach electrodes in the electrical circuit can be registered as an evidence of particle arrival in the selected volume.

Voltage applied to the electrodes is selected with the approach so the newly generated ions run to according electrodes fast enough to not start recombination process and not too fast to break other atoms of matter to ions or in other words not to generate

secondary ionization process. If particle trail is entirely fits in volume of detector full ionization energy caused by the particle can be achieved.

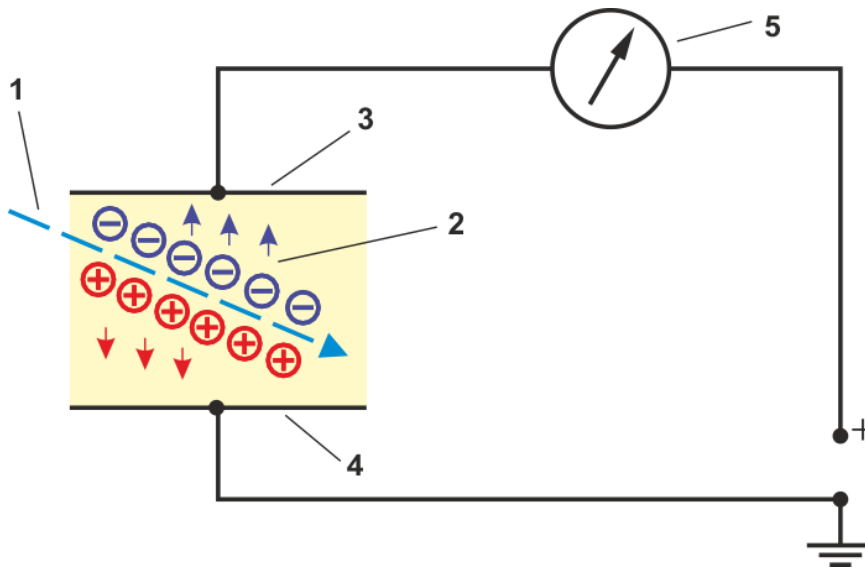


Figure 7. Scheme of ionization chamber

- 1 – trajectory of a particle; 2 – positive and negative ions caused by particle;
 3 – positive electrode; 4 – negative electrode; 5 – current registry device.

There are two main types of ionization chamber: integration and impulse. Integration chamber measures summary ionization current. Impulse chambers detects single particle and measures its energy.

Integration chambers is more simplify because value of its measurements is rather high then those in impulse chambers.

To measure a signal going through the circuit when particle hit the volume of detector we can imagine detector volume as a capacitor so newly generated ion charges will cause difference of voltage.

$$\Delta U = \frac{Q}{C} \quad (1)$$

where C is capacity of the chamber, and ΔU is difference of voltage that can be measured with registry device, Q is summary charge of ions passing through the circuit.

Those ions are generated by the ionization process so the number of ion pairs can be calculated by the following equation:

$$n = \frac{E}{I} \quad (2)$$

where E is energy of particle, I – is energy consumed per ion pair generation.

By multiplying this number of pairs on elementary charge summary charge can be found. So we can assume equations (1) and (2) to the following equation:

$$\Delta U = \frac{Ee}{CI} \quad (3)$$

where e – is elementary charge has a measured value of approximately $1.602176565(35) \times 10^{-19}$ coulombs.

In summary can be said that impulse measured is proportional to the energy of particle. If energy consumed per pair is known for particular matter energy of the particle can be achieved.

Gaseous ionization detectors have the same general principle as ionization chamber. Sensitive matter is gas with applied voltage and difference of voltage recorded by registry device is an evidence of particle passing through the volume of detector. Main difference and feature of gaseous detector is that it uses secondary ionization processes for signal amplification.

Gaseous counters are grouped as **proportional counters** and **Geiger-Müller counters**.

Proportional counter has dependent discharge that means that it attenuates without external ionization. In Geiger-Müller counter has independent discharge so process of secondary ionization repeats continuity and it has to be stopped manually.

Proportional counters designed as hermetic chamber with thin walls made of glass and usually has form of tube. Inner side of glass is covered with metal that acts as cathode. Anode is thin metal wire in the center of tube. Such asymmetrical configuration determines main features of this detector. Scheme is shown at the following figure.

Electrical field in the closest area to wire is rather higher than one in remain volume of chamber. It results in several specific physical processes taking place in the volume of gaseous detector.

Primary ionization: Emerges in the way of charged particle passing through the volume of counter. It is worth to mention that primary ions can arrives at any place in the tube of counter. If trajectory of particle fully fits inside the tube number of ions is proportional to energy of particle.

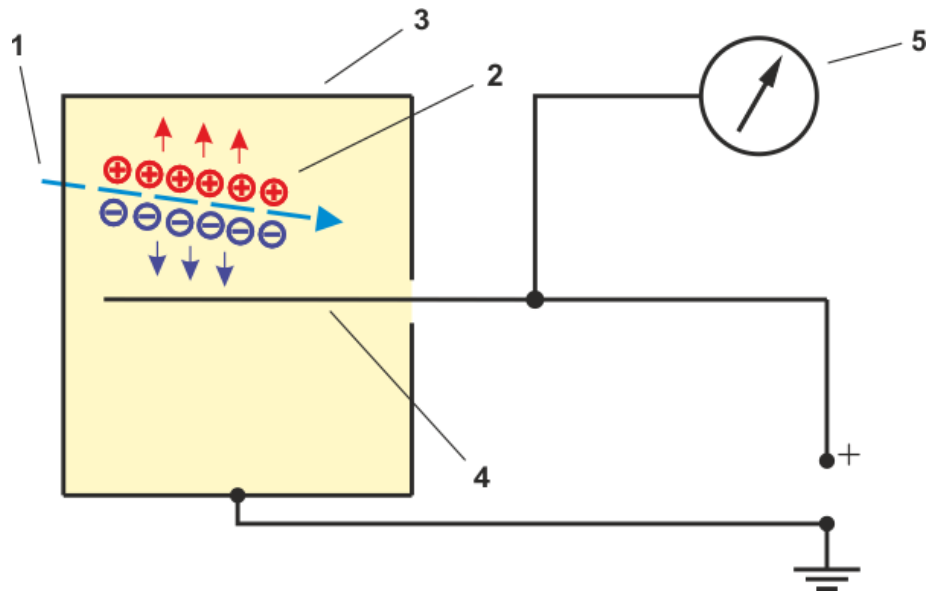


Figure 8. Scheme of gaseous counter

- 1 – trajectory of a particle; 2 – positive and negative ions caused by particle;
 3 – negative electrode; 4 – positive electrode; 5 – current registry device.

Secondary ionization: Primary electrons and positive ions accelerated by electrical field and starts to move to electrodes in the same way as at ionization chamber. However cause of asymmetrical structure of tube further developments goes in other scenario. Electrons move to the anode-wire and arrive in area of high electrical field (electric lines of force go radically around wire and field becomes stronger in the close area to the wire) and accelerates very rapidly at the center of tube. As result secondary wave of ionization arises. Electrical field is strong enough that newly generated electron is possible to cause another ionization process, so the process becomes avalanche like. One primary electron can produce hundred thousand or even more secondary particles. There are two main features of avalanche process. First is that secondary ionization happens in very small area (about 10^{-2}sm) around wire. Volume of this area is far smaller than rest of detector's volume. It can be considered that primary ionization always happens out of this area and thus every primary electron generates same number of secondary waves. Because number of primary electrons is proportional to energy of the particle overall number of generated particles is also proportional to its energy. Second feature of avalanche process is very small duration (about 10^{-8}s).

Avalanche processes. After primary avalanche in counter can occur sub avalanches. Sub avalanches can be caused by two different mechanisms. First mechanism is related to

fast processes those happens at the start of avalanche process. Electrons cause molecular excitation that results in photons emergency. Photons knock out new electrons from cathode those starts new avalanche process. Duration of such process can be estimated as 10^{-6} s if assume that size of tube equal to 1cm (when velocity of electron 10^6 cm/s). Second mechanism related to much slower processes. Positive ions arrived at cathode knock out new electrons as result of neutralization. Because energy that exposed in cathode by ion of gas is greater than ionization energy of cathode matter. So duration of such process is determined by speed of ions (10^4 cm/s) and can be estimated as 10^{-4} s. If mentioned mechanism can cause sub avalanches for indeterminate amount of time discharge can be treated as independent. Such discharge can be induced if high voltage was applied to the counter.

Geiger-Müller counter. Counter of this type deal with independent discharge and has rather high impulse that is not depend on energy of registered particle. So this counter only registers particle emergence and doesn't provide information about its energy. Time resolution of such counter is also greater than one at proportional counters, usually 10^{-3} - 10^{-5} s (superior 10^{-8} s).

Most important feature of Geiger-Müller counter is *counter characteristic* that is responsible for number of counting in dependant of voltage applied. This characteristic has a curve with wide horizontal part that is called *plateau* and it is working area of counter. The wider working area the better quality of counter. Counter characteristic of Geiger-Müller counter is shown at the following figure.

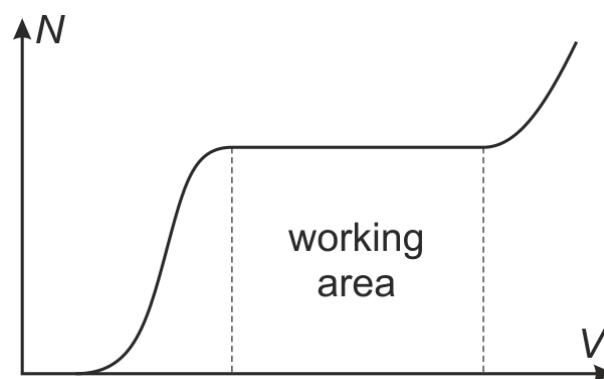


Figure 9. Counter characteristic of Geiger-Müller counter

Dependence between number of pulses N and voltage applied V at a constant intensity

Effectiveness of charged particle registration for Geiger-Müller counter is also proximal to 100%. Geiger-Müller counter is well designed, cheap and very easy to operate. That is why such counters are widely used in applied nuclear physics. But in purpose of science more precise devices are used.

Scintillation counter. This counter consists of substance that is able to cause excitation under effect of incident radiation that result in light pulses. Light pulses were used for charged particle registration at the dawn of nuclear physics. As scintillator material was used zinc sulphide ZnS and number of flares caused by particles were counted with the naked human eye.

Nowadays as a sensitive matter used materials those are transparent to own scintillation emission. So all volume of scintillator can be effectively used for registration instead of zinc sulphide where only surface was used. As registry device photoelectric electron-multiple tubes (PMT) are used nowadays those have rather high response time in comparison to human eye.

Scheme of common scintillator detector is shown at the following figure. When particles pass through the volume of scintillator matter, its atoms are excited that results in photon emitting. Duration of this process can be estimated as $2 \cdot 10^{-7}$ s. Photons passing through light pipe hits photocathode causing photoelectron emission. After that electrons those pass through focusing tool strikes first dynode. Material of dynode chosen by its ability to cause secondary electron emission. So beam of electrons after each hit of the next dynode is amplified with bunch of new electrons. Each electron generate 6-10 new at every hit. If take into account that in common scintillator detector used from 10 to 20 dynodes it allows to amplify beam of electrons by 10^5 - 10^8 . At the last hit beam of electrons arrives at anode causing electrical impulse that can be registered by mentioned radiotechnical methods.

Advantage of scintillator detector is approximately 100% effectiveness of charged particles detection. And that it has very small time resolution that is dependant on duration of light pulse. Duration can vary of material used as scintillator, for nonorganic crystals it is about 10^{-7} s, for organic approximately 10^{-8} s, and plastic scintillator can decrease time resolution down to 10^{-9} s. Other advantage of this type of detector that it allows not only register a particle but also to measure its energy and even velocity. For this purpose a thin crystal is used. When particles pass through it, energy loss can be measured that is velocity difference in other words.

Disadvantage of this detector is that scintillator material is very hygroscopic and is sensitive to strong light beams. So sensitive matter of scintillator detector have to be carefully protected from moisture and direct light.

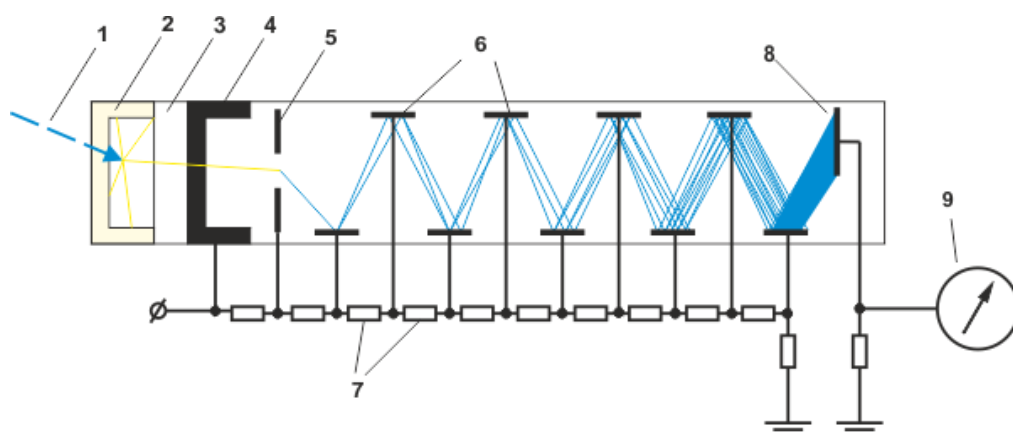


Figure 10. Scheme of scintillation counter

- 1- particle trajectory, 2 – scintillator, 3 - light pipe, that connects scintillator and PMT,
- 4 – photocathode, 5 – focusing tool, 6 – dynodes, 7- potential dividers, 8 – anode,
- 9 –registry device, photoelectrons generation trajectories are shown with blue lines.

Wilson cloud chamber. The cloud chamber, also known as the Wilson chamber, is a particle detector used for detecting ionizing radiation.

Most common cloud chamber is a sealed volume that contains supersaturated vapor of water or alcohol. When charged particle pass through volume of detector it ionizes fluid. Generated ion pairs act as base body for condensation process that results in mist forming on the way of particle. The high energies of alpha and beta particles mean that a trail is left, due to many ions being produced along the path of the charged particle. These tracks have distinctive shapes (for example, an alpha particle's track is broad and shows more evidence of deflection by collisions, while an electron's is thinner and straight). When any uniform magnetic field is applied across the cloud chamber, positively and negatively charged particles will curve in opposite directions, according to the Lorentz force law with two particles of opposite charge.

Methanol vapor saturates the chamber. The alcohol falls as it cools down and the cold condenser provides a steep temperature gradient. The result is a supersaturated environment. The alcohol vapor condenses around ion trails left behind by the travelling ionizing particles. The result is cloud formation, seen in the cloud chamber by the presence of droplets falling down to the condenser. As particles pass through they leave ionization

trails and because the alcohol vapor is supersaturated it condenses onto these trails. Since the tracks are emitted radially out from the source, their point of origin can easily be determined.

Just above the cold condenser plate there is an area of the chamber which is sensitive to radioactive tracks. At this height, most of the alcohol has not condensed. This means that the ion trail left by the radioactive particles provides an optimal trigger for condensation and cloud formation. This sensitive area is increased in height by employing a steep temperature gradient, little convection, and very stable conditions. A strong electric field is often used to draw cloud tracks down to the sensitive region of the chamber and increase the sensitivity of the chamber. While tracks from sources can still be seen without a voltage supply, background tracks are very difficult to observe. In addition, the voltage can also serve to prevent large amounts of "rain" from obscuring the sensitive region of the chamber, caused by condensation forming above the sensitive area of the chamber. This means that ion trails left by radioactive particles are obscured by constant precipitation. The black background makes it easier to observe cloud tracks.

Before tracks become visible it is necessary to illuminate it with light source. So it become visible more clearly black material is usually added on background. Tracks from particle should be viewed from horizontal position if chamber parameters were set correctly. The tracks become much more obvious once temperatures and conditions have stabilized in the chamber. This requires the elimination of any significant drift currents (poor chamber sealing).

Bubble chamber. A bubble chamber is a vessel filled with a superheated transparent liquid (most often liquid hydrogen) used to detect electrically charged particles moving through it. It was invented in 1952 by Donald A. Glaser, for which he was awarded the 1960 Nobel Prize in Physics.

Cloud chambers work on the same principles as bubble chambers, but are based on supersaturated vapor rather than superheated liquid. While bubble chambers were extensively used in the past, they have now mostly been supplanted by wire chambers and spark chambers. Historically, notable bubble chambers include the Big European Bubble Chamber (BEBC) and Gargamelle.

The bubble chamber is similar to a cloud chamber, both in application and in basic principle. It is normally made by filling a large cylinder with a liquid heated to just below its boiling point. As particles enter the chamber, a piston suddenly decreases its pressure,

and the liquid enters into a superheated, metastable phase. Charged particles create an ionisation track, around which the liquid vaporises, forming microscopic bubbles. Bubble density around a track is proportional to a particle's energy loss.

Bubbles grow in size as the chamber expands, until they are large enough to be seen or photographed. Several cameras are mounted around it, allowing a three-dimensional image of an event to be captured. Bubble chambers with resolutions down to a few μm have been operated.

The entire chamber is subject to a constant magnetic field, which causes charged particles to travel in helical paths whose radius is determined by their charge-to-mass ratios and their velocities. Since the magnitude of the charge of all known charged, long-lived subatomic particles is the same as that of an electron, their radius of curvature must be proportional to their momentum. Thus, by measuring their radius of curvature, their momentum can be determined.

Spark detector. A spark chamber is a particle detector that combines benefits of immediate registration and fullness of information that can be achieved by track detectors. Operating principle of this detector is based on spark discharge that emerges in gas when ionizing particle pass through its volume. Most simplest spark chamber consist of two orthogonal electrodes with gas (usually Ne, Ar or its mix) in the volume between. Electrodes area can vary from several square dm to several square meters. Simultaneously with signal from counter detector (scintillation counter or others) or with delay to electrodes are applied short (10-100ns) pulse of high voltage (5-20kV/cm). Electrons caused by ionization process accelerated by strong electrical field cause wave of electron-photons avalanches those grows to the level of visible spectrum.

Electrodes are located on distance of 1cm from each other. Half of them are connected to ground wire and to half of them high voltage is applied. Chain of sparks between electrodes draws particle trajectory with approximately to parts of millimeter accuracy. Time resolution is approximately 10^{-6}s , and full reset time is about 10^{-3}s . Those detectors are able to detect particles with inlet angle up to 50° . For tracking particles with higher inlet angles special streaming mode is used. Streaming chamber is subtype of spark chamber those uses more short pulses with duration 10ns. As result trajectory of particle passing through the volume of chamber can be seen as chain of separate dots.

Tracking spark chambers have high effectiveness and are able to register several particles at same time. As was mentioned this detector is not independent and other counter detectors have to be used to detect particle emerge first.

Proportional chamber. A multi-wire proportional chamber is a type of proportional counter that detects charged particles and is able to provide information about its trajectory.

The multi-wire chamber consist of two orthogonal rows of wires with high voltage applied to one row, and other row is connected to the ground. The chamber is filled with gas (argon/methane mix), such that any ionizing particle that passes through the volume of detector starts ionization process in matter of detector. Generated ion pairs are accelerated by the electric field around the wire, causing processes of secondary ionization avalanches. Generated ions are collected on the nearest wires that results in a charge proportional to the ionization effect of the detected particle. By computing pulses from all the wires, the particle trajectory can be found.

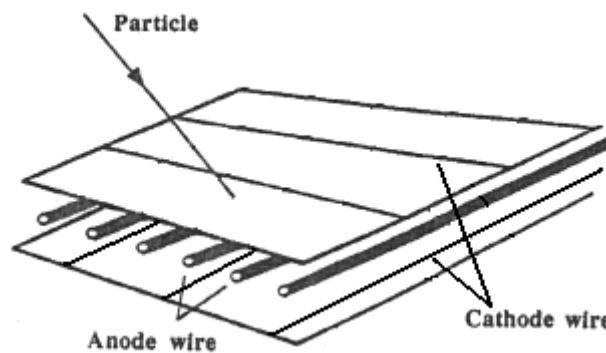


Figure 11. Scheme of proportional chamber

Semiconductor detector. Internal design of this detector is quite similar to the one at ionization chamber. Instead of gases this detector uses solid as ionization matter. Advantage of this detector is that depleted layer where process of ionization take place generates more ions and small size of detector's volume allow rather highest spatial (about 1mm) and time resolution (10^{-9} s).

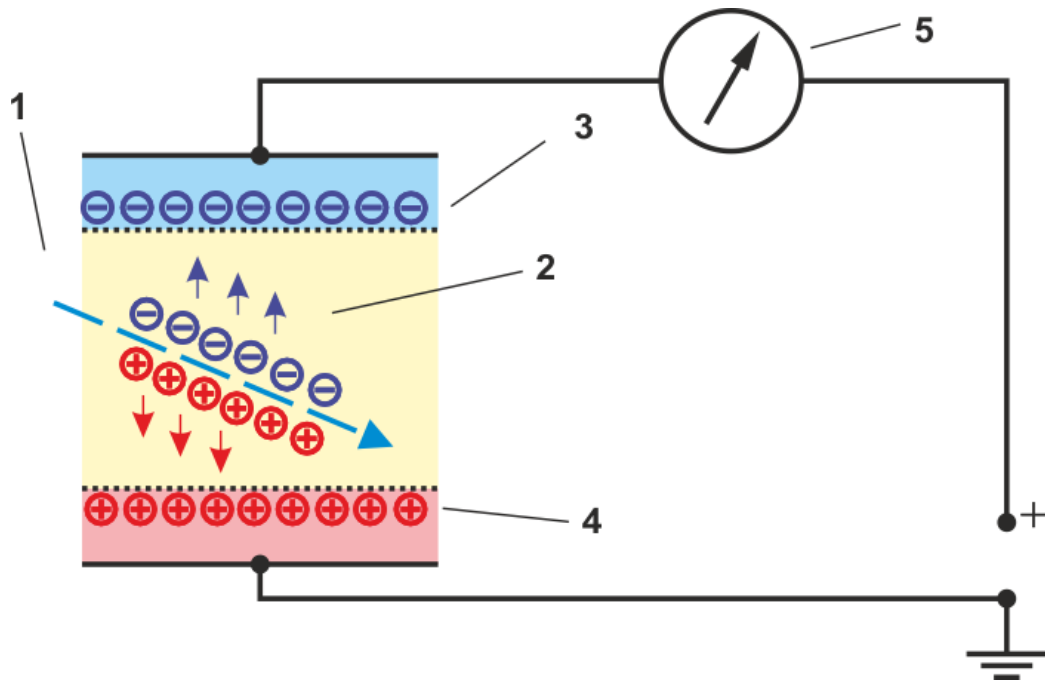


Figure 12. Scheme of Semiconductor detector

1 – trajectory of a particle; 2 – positive and negative ions caused by particle in depleted layer ;
 3 – positive electrode; 4 – negative electrode; 5 – current registry device.

Relations (3) described above for ionization chamber can be used for semiconductor detector.

Pixel detector (semiconductor type). Pixelated silicon detectors are used in experiments at the LHC.

As sensitive part semiconductor sensor is used. Each semiconductor has its own cheap. Sensitive units composed in large 2d dimensional array. Scheme of such detector can be seen at the following figure.

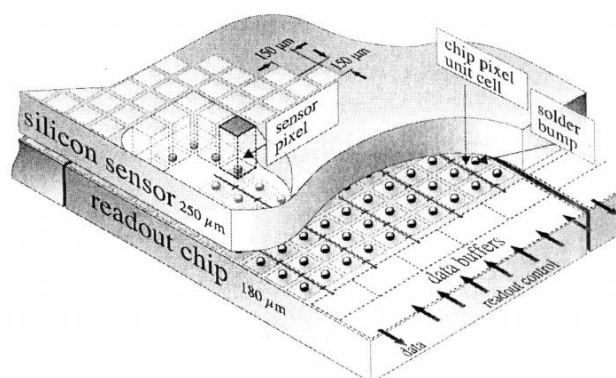


Figure 13. Scheme of Pixel detector

Detector part selection justification

Main characteristics of all above mentioned can be converged to the following table:

Table 1. Main characteristics of existing particle detectors

Detector type	Dimensional resolution, cm	Time resolution, s	Reset time, s
Ionization chamber	~1	10^{-6}	10^{-4}
Proportional counter	~1	10^{-7}	10^{-5}
Geiger-Müller counter	~1	10^{-9}	10^{-4}
Scintillation counter	~1	10^{-9}	10^{-8}
Semiconductor detector	<1	10^{-9}	10^{-9}
Wilson cloud chamber	10^{-1}	10^{-1}	10^{-3}
Bubble chamber	10^{-2}	10^{-3}	1
Spark detector	10^{-2}	10^{-6}	10^{-3}
Proportional chamber	10^{-2}	10^{-7}	10^{-5}

As can be seen from the table above detectors those fulfill conditions of the task by dimensional parameters are all types of tracking detectors and semiconductor detector. But most of tracking detectors don't meet requirements of the task by time parameters. Assignment, inner design and information release process of tracking devices doesn't allow to use it in the purpose of current work. It follows thence that within the bounds of the task from all of the mentioned above detectors only semiconductor type detector can be used, that was namely recommended for application in the technical task. It is worth mentioning that professional decisions in area of particle detectors for example pixel detector that is also based on semiconductor technology can be also used in the purpose of this work. But the fact that semiconductor will unavoidably degrade in conditions of frequently usage and because of high cost of pixel detector it is rational to use simple semiconductor detector that can be rapidly changed.

It was decided to use as sensitive unit in semiconductor detector a Si diode. Its wide occurrence and low cost are allow using it as sensitive unit in replaceable detector part of device. Detector part is silicon slice with conductive coatings and several (4-8) diodes soldered to it.

Scheme of sample and store

Charged particle passing through junction depletion zone of semiconductor unit causes amount of ion-pairs. Those ions under effect of back voltage applied to the junction flows to terminals of current supply unit. Current caused by those ions is proportional to the number of ion pairs passing through the junction zone per unit time and size of the junction zone accordingly. In the way of diode usage size of junction zone is quite uncertain value so sensitivity of detector based on such diodes can be obtained experimentally. It is not possible to measure immediate current but we can measure charge for a an interval of time as a potential that has been stored at capacitor. It can be done using following equation:

$$Q_c = \frac{1}{C} \int_{t_1}^{t_2} i(t) dt \quad (4)$$

where t_1 – start time, t_2 – end time, C – capacity of used capacitor.

As can be seen from mentioned equation potential from diode is proportional to current and negatively related to the capacitance of capacitor. Value of capacitance determine sensitivity of all scheme. Un this case scattering of capacitors nominal brings additional contribution to the heterogeneity of used multichannel system alongside with scattering of diodes sensitivity.

Charge accumulated at the capacitor has be saved in period of time necessary to make its analog to digital conversion (ADC). It can be done using following scheme with several analog switches and capacitor as shown at the following figure.

When switch (3) and (2) are closed current supply is connected to the ground through the switch (3) and capacitor (4) discharges to zero potential through switch (2). When switch (3) is opened and switch (2) is closed current supply starts to charge capacitor. If switch (2) is off and switch (3) is on current supply is connected to the ground and capacitor is storing accumulated charge.

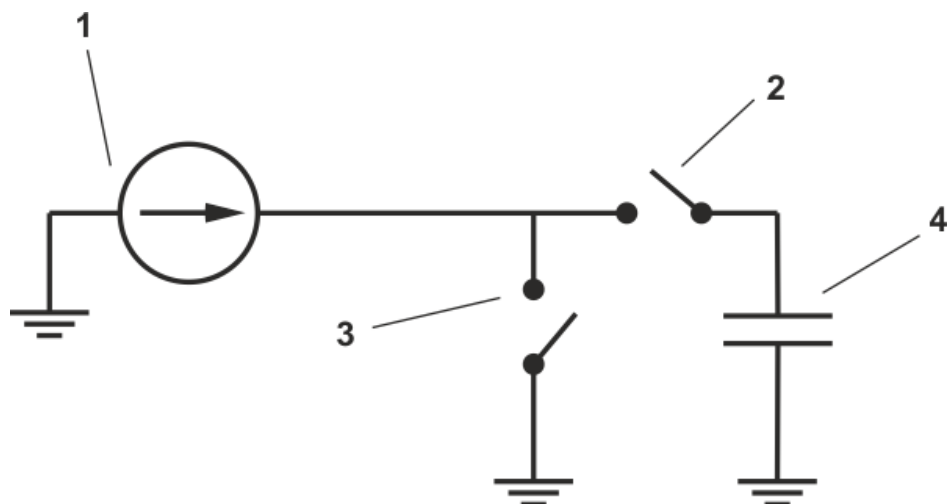


Figure 14. Non-inverted sample and store schematic

1 – positive current supply; 2 – switch (2); 3 – switch (3); 4 – capacitor.

It is also possible to use another schematics drawn at the following figure.

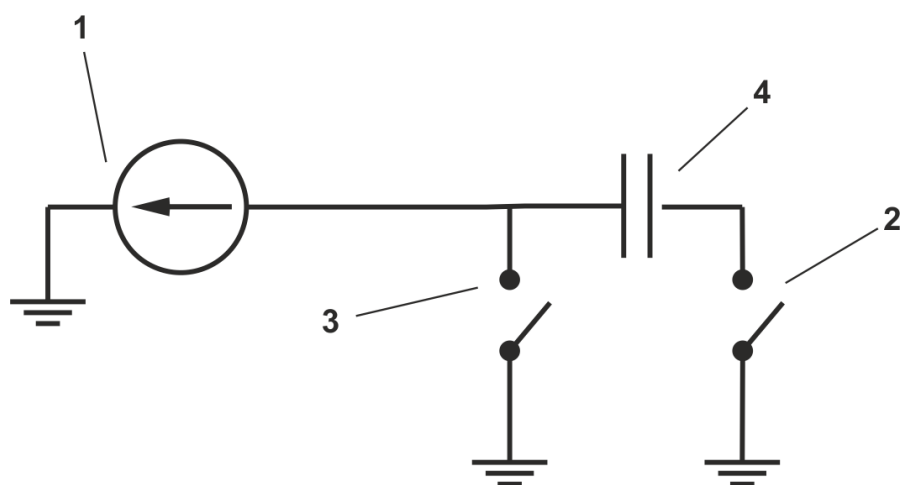


Figure 15. Inverted sample and store schematic

1 – negative current supply; 2 – switch 1; 3 – switch 2; 4 – capacitor;

At this scheme storage capacitor is connected between two switches those terminated to the ground.

Working algorithm of this scheme is following: when switches (3) and (2) are closed current supply is connected to the ground and capacitor charges to the zero potential. If switch (3) is opened and switch (2) is closed capacitor charges by current of

supply. When switch (2) is off and switch (3) is on current from current supply flows to the ground and capacitor (4) stores accumulated charge.

Feature of this schematics is inversion of output voltage in relation to the input current.

In case of inverted polarity of current, supply voltage on the right coat of capacitor will be positive. This determines the possible application of mentioned scheme. Because common ADC works with positive voltages so this scheme can be used for negative power supplies.

In our case current from detector depends on polarity of diode connection and polarity of voltage supply. But it is easier in purpose of our task to work with positive voltage supply so first schematics will be used.

Analog switch controlling microchip

As microchip for analog switch control was selected microchip ADGx series (ADG511/ADG512/ADG513) manufactured by Analog Devices. Main features of chip are described below:

Features

+3 V, +5 V or 5 V Power Supplies

Ultralow Power Dissipation (

Low Leakage (<100 pA)

Low On Resistance (<50 Ohm)

Fast Switching Times

Low Charge Injection

TTL/CMOS Compatible

16-Lead DIP or SOIC Package

Inner scheme of microchip is shown at the following figure:

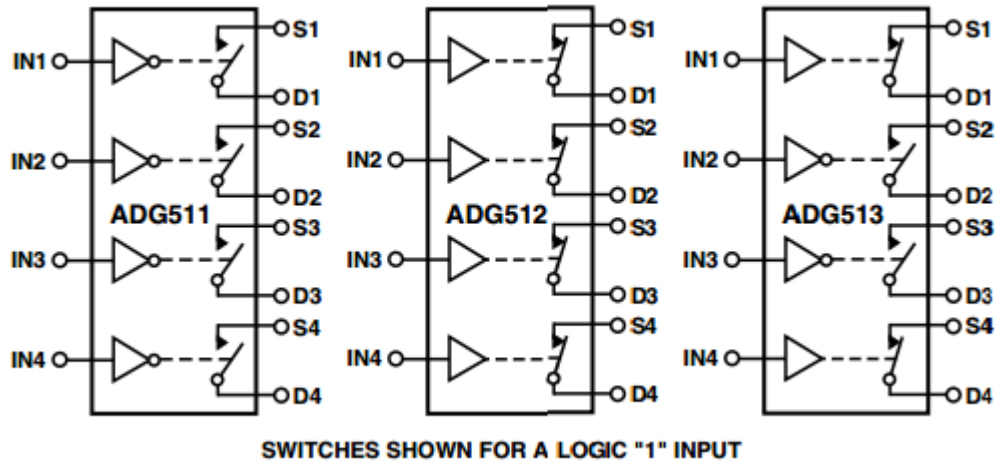


Figure 16. Analog switch controlling Microchip ADG51x series

Most important feature in purpose of our task is low leakage current (<100 pA) and ability to work with single supply voltage +5V. For this task microchip ADG512 was selected as most suitable. At the next chapter simulation in circuit simulation program (MicroCap 9) of such schematics for a single sensitive unit will be described in details.

Sensitive unit work cycle description

Electrical charge flowing from the semiconductor sensitive unit to the registry device as follows from equation (3) is proportional to the number of proton particles, passing through the junction depletion zone. Measuring of beam intensively is achieved by integration of the current of semiconductor unit (diode) on the storage capacitor with subsequent analog to digital conversion of voltage difference on the MCU leg. Scheme of single sensing channel is shown at the following figure. Sensitive unit (diode) is shown at the scheme as pulsed current source I1 (because complicated process of ionization that take place in diode under irradiation cannot be simulated in common circuit simulation program) with following parameters:

1. Amplitude of the current impulse - $1 \mu\text{A}$;
2. Impulse duration - $1 \mu\text{s}$;
3. Pulse period - $25 \mu\text{s}$.

Those parameters are taken accordingly to parameters of proton beam [1].

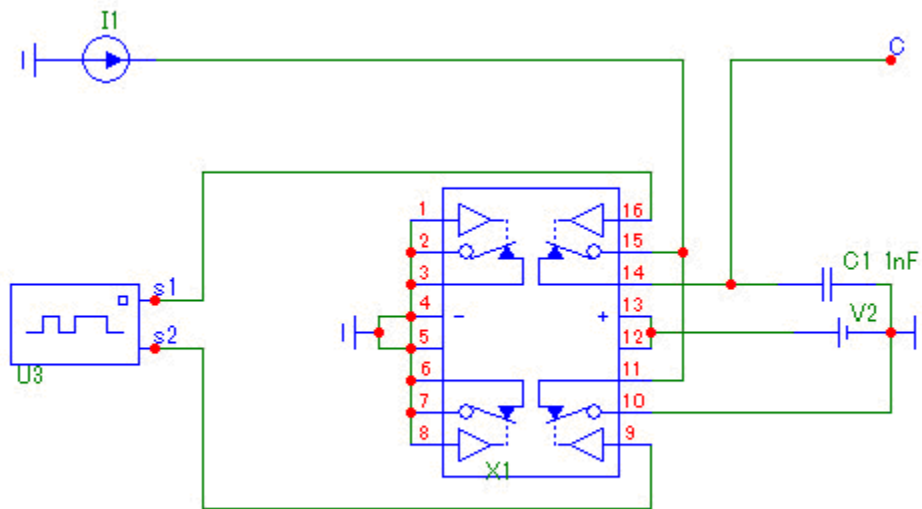


Figure 17. Scheme of single sensitive unit circuit

I1 – power supply (irradiated diode), C1 – storage capacitor, X1 – chip with 4 switches (only 2 are used for a single channel), U3 – switches controlling signals from MCU, V3 – 5V power supply from MCU, C – signal to MCU.

Note: All legs of left side of switch chip X1 are grounded. It was made in purpose of scheme simplification and requirements of the circuit simulation program. In real circuit left part is responsible for other channel and all connections are symmetrical to the right side.

There are 2 analog switches in the scheme those are present in inner design of chip X1 (ADG512BR). First switch (at leg 15) switches off/on storage capacitor C1 to the supply source I1 (irradiated diode). Second (at leg 10) switch closes supply source current to the ground and also allows discharge of storage capacitor when first switch is closed. From 4 possible combinations of switch conditions (on/off) only 3 are allowed in work cycle, more specifically following:

1. First on, second off – charging of capacitor C1;
2. First off, second on – storage of the charge on the capacitor;
3. First on, second on – discharge of capacitor C1.

Fourth condition (both switches are off) is used shortly to remove steady leakage current through the switches.

Working cycle of switches are controlled the MCU (ATMEGA328P) with signals s1 and s2. At the scheme control signals from MCU are shown as block U3.

There are 2 possible working modes: synchronous and asynchronous.

At the synchronous mode additional sync signal are used. This signal is followed immediately by beam pulse. At the following figure results of signal simulation in circuit program as a timing diagram are shown. Top diagram represents pulses of proton beam with 25ms period and duration 1ms. Next 2 diagrams are switch controlling signals from MCU. Bottom diagram represents voltage at storage capacitor C1. Synchronization pulse is not shown but as can be seen controlling signals are linked to the beam pulses.

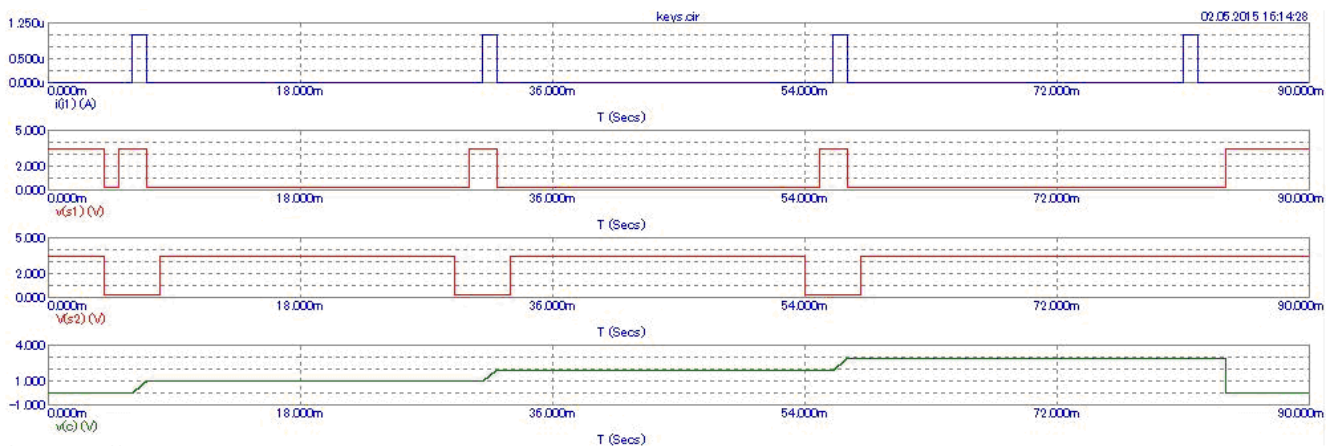


Figure 18. Timing diagram of sensitive unit duty cycle in synchronous mode

Intensively of the beam is slightly different from pulse to pulse (about 5% [1]), so averaging of measurements by several pulses has to be applied. It is worth mentioning that

mechanical part doesn't allow movements of detector part in such a short period of 25ms. So charge storage for a several beam pulses is used. Number of pulses can be assigned by the program.

As can be seen from diagram capacitor charging occurs with 3 consequent pulses of the beam. After third pulse circuit stands in storage mode. Long time interval of storage mode is used for analog to digital conversion of signal read by MCU. After that discharge of the capacitor occurs. Synchronous mode allows minimal charge leakage from capacitor, but requires input of synchronization signal. But if take to account that number of charge periods in real conditions can be more then 3 (10-20) it allows to cancel usage of synchronization channel. In this way asynchronous mode can be implemented. Simulated diagrams of this mode can be seen at the following figure.

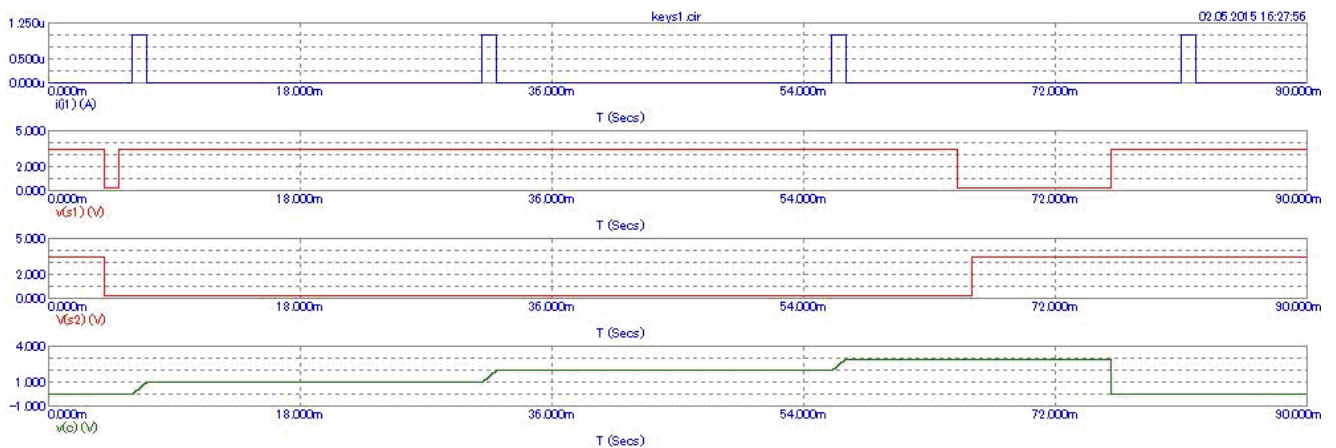


Figure 19. Timing diagram of sensitive unit duty cycle in synchronous mode

Main difference of this mode from previous one that first switch is still closed and second opened at the whole period of time multiple to the number of beam pulses. After that circuit goes consequently to the storage mode and discharge mode.

Sample and store possible modifications

There are to possible modifications of Sample and Store block in dependence of MCU used. Atmega 328P has embedded multiplexor for 8 analog channels, however arduino Nano that has the same MCU and 8 analog inputs but arduino Uno has only 6 analog inputs that is not enough for us. So external multiplexor is required for arduino Uno to meet demands of our task.

However arduino Uno has ability to connect compatible shield for stepper motors and nano does not.

There were 2 available ways: develop a board with multiplexor for arduino Uno and develop board for stepper motor control that can deal with arduino Nano. I decided to make both. There are 8 channel Sample and Store block for arduino Nano and 16 channel block with multiplexor for arduino Uno modifications used in those project. Second was selected as preferable by director of enterprise. Advantage of using arduino Uno is also the fact that it can use 20V voltage level as input supply. This particular voltage level is also used as blocking voltage in scheme of sensor part (20V voltage level was recommended as blocking voltage by several publications related to this work [1] and [3]).

Mechanical part

Translation movement

Mechanical part of device is represented by 2 independent translation axis, driven by 2 low voltage bipolar motors. Rotor of the motor is manufactured as a part of a shaft for screw drive. Characteristics of the motor are listed in the following table.

Table 2. Motor specification:

Motor type:	2-phase 4-wire
Driving voltage:	DC4-6V
Screw length	74.8
Screw pitch:	3mm
Step angle:	18 °

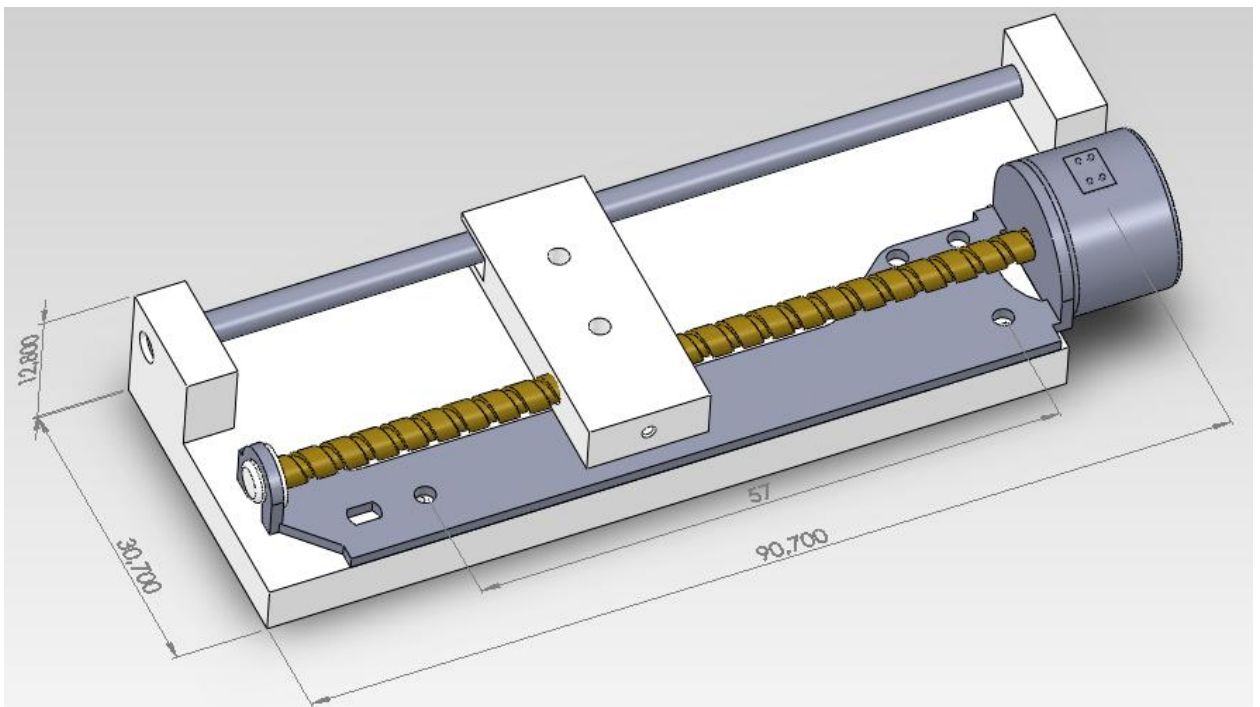


Figure 20. Motor with screw-shaft rotor

Minimal translation movement by axis can be calculated by the following equation:

$$X_{\min} = \frac{\alpha}{360^\circ} \cdot pitch$$

where α - angle step, pitch – distance between 2 adjacent coils of screw

For these motors minimal translation step will be:

$$X_{\min} = \frac{18^\circ}{360^\circ} \cdot 3mm = 0,15mm$$

So minimal translation movement for this motor is 0.15mm that is enough for this task.

Weight of sensor unit is far less than weight of motor's assembly nut so all calculations of required torque were considered unreasonable.

Null detectors of zero position detectors are fixed in the corners at each stepper (aren't shown at the figure above) . Detectors allow to determine if detector in “parking zone” or not.

Control part

Algorithm of reconstruction of beam spatial distribution

Main task of the developed device is to check if parameters of beam are correct. Correct beam is considered as beam with form close to circle and spatial distribution close to normal distribution with size 5.5-6mm on 50% dose. Those parameters were set as optimal for purpose of proton therapy and all medical calculations were made according to this size of beam. With relation to the fact that near correct parameters of beam are achieved by the measuring (ionization and proportional chambers) and controlling devices (magnetic lenses) located on the way to the area of irradiation the task of developed device is to perform final settings in the immediate area of irradiation. Spatial distribution of particles in the beam in the area of irradiation has to be close to normal already. The task is to reconstruct it by scanning cross section of the beam with 2 orthogonal rows of semiconductor sensor. Because approximate position of beam is already known, 8 (4 in other case) sensitive units located in distance of 1 mm from each other has to be set immediately near the center and achieve information about intensity as slices of beam on each axis with 1 mm step between slices and 0.2mm discretization in each slice.

To examine algorithm lets simulate it MatLab environment. As soon as beam conform the law of normal distribution, intensively of particles in beam cross section can be represented as 2 dimensional Gaussian. 3d representation of the beam spatial distribution and positions of sensitive units in relation to it can be seen the following figure.

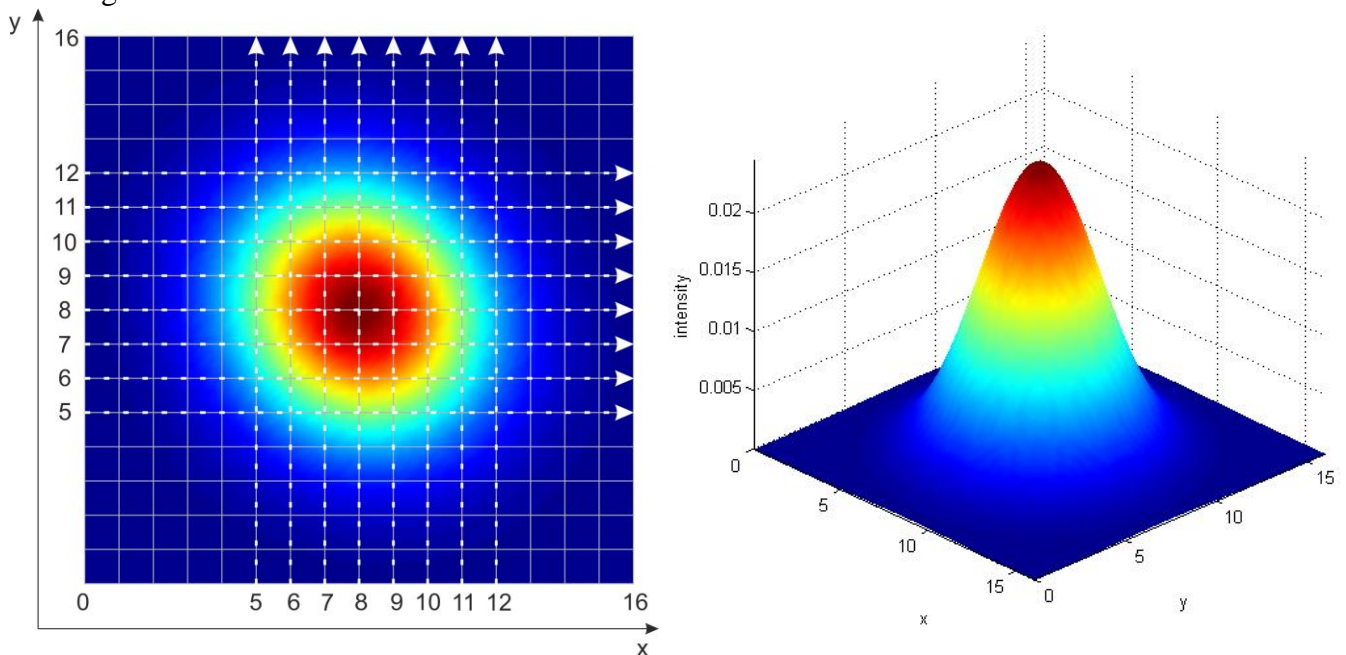


Figure 21. Mathematical representation of spatial distribution of particles in the beam.

Position and translation movements of sensitive units is shown as white arrows. Intensity of particles in proton beam represented as z coordinate of surface and color differences.

MatLab script simulates process of reconstruction Gaussian from noised data achieved from 2 orthogonal detectors. Each detector has 8 diodes with different sensitivity ($\pm 20\%$). Here is code of the script with comments:

```
step=16/80;           %step of translation movement of detector
x=(0:step:16);       %X axis of working area 16mm divided by step
y=x;                 %same for Y axis
```

Mathematical parameters of normal distribution. Point of maximal intensity (8;8) and standard deviations calculated by taking into account that size of beam should be approximately 6mm on 6mm on 50% dose. Ratio between full width at half maximum and standard deviation is 2.355. 2d Gaussian surface can be obtained using following equation:

$$f(x, y) = \frac{1}{2\pi\sigma_x\sigma_y\sqrt{1-r_{xy}^2}} e^{-\frac{1}{2(1-r_{xy}^2)}\left[\frac{(x-m_x)^2}{\sigma_x^2} - \frac{2r_{xy}(x-m_x)(y-m_y)}{\sigma_x\sigma_y} + \frac{(y-m_y)^2}{\sigma_y^2}\right]}$$

m_x - mean by X axis; m_y - mean by Y axis, r_{xy} - correlation coefficient, σ_x - standard deviation by X axis; σ_y - standard deviation by Y axis; x - coordinate of diode by X axis in X-scanning row; y - coordinate of diode by Y axis in Y-scanning row.

```
Rxy=-0.1;           %correlation coefficient
FWHWx=6;           % full width at half maximum by X axis
FWHWy=6;           % full width at half maximum by Y axis
Sx=FWHWx/2.355;    %standard deviation X axis
Sy=FWHWy/2.355;    %standard deviation Y axis
Mx=8;              %mean by X axis
My=8;              %mean by Y axis
```

Drawing Gaussian that shown at figure above.

```
[xx,yy]=meshgrid(x,y);
%creates normally distributed intensity with mentioned parameters
h=1/2/pi/Sx/Sy/sqrt(1-Rxy*Rxy)*exp((- (xx-Mx) .* (xx-Mx) /Sx/Sx- (yy-My) .* (yy-My) /Sy/Sy+2*Rxy*(xx-Mx) .* (yy-My) /Sx/Sy)*0.5/(1-Rxy*Rxy));
surf(xx,yy,h);      %draw Gaussian surface
shading interp
axis tight
view(0,90)
```

```

xlabel('x');
ylabel('y');
zlabel('intensity')

```

For simulation data achieved from diodes slices of Gaussian surface can be taken at corresponding coordinates.

```

posX=(5:1:12);      %distance between diodes by X axis
posY=(5:1:12);      %distance between diodes by Y axis

dX=posX/step;       %step movements of diodes by X axis
dY=posY/step;       %step movements of diodes by Y axis

sliceY=zeros(81,8); %for storing data of "ideal" data from Y
diodes
sliceX=zeros(8,81); %for storing data of "ideal" data from Y
diodes

%getting "ideal" data as slices from Gaussian surface
for i=1:1:8          %slicing "ideal" data from Gaussian
    sliceY(:,i)=h(:,dY(i));
end
sliceY=sliceY';

for i=1:1:8          %slicing "ideal" data from Gaussian
    sliceX(i,:)=h(dX(i),:);
end

```

Adding amplification to signals that represents sensitivity scatter of sensor units ($\pm 20\%$) and random white noise.

```

a=0.8;              %min sensitivity
b=1.1;              %max sensitivity

kdX=a+(b-a)*rand(1,8); %diodes sensitivity amplification on X
axis
kdY=a+(b-a)*rand(1,8); %diodes sensitivity amplification on Y
axis

noise=25;           %noise level in decibel

sliceXa=sliceX;
for i=1:1:8          %slices of "real" data with noise and
amplification
    sliceXa(i,:)=awgn(sliceX(i,:)*kdX(i),noise,'measured');
end

sliceYa=sliceY;
for i=1:1:8          %slices of "real" data with noise and
amplification

```

```

sliceYa(i,:) = awgn(sliceY(i,:) * kdY(i), noise, 'measured');
end

```

For better understanding simulated data can be drawn.

```

figure1 = figure
surf(xx, yy, h, 'facealpha', 0.5)
shading interp
axis tight
xlabel('x');
ylabel('y');
zlabel('intensity')
hold on
for i = 1:1:8
    plot3(x, yy(dX(i)), :, sliceX(i,:), '--b')
end

for i = 1:1:8
    plot3(xx(:, dY(i)), y, sliceY(i,:), '--b')
end

```

Result is shown on the following figure.

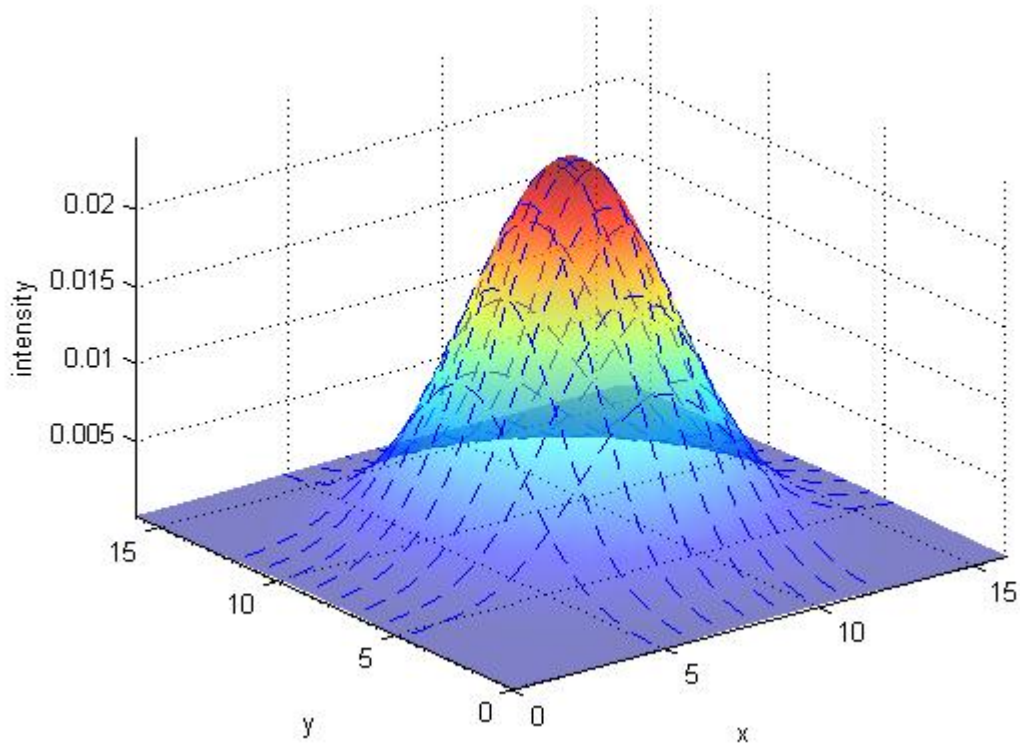


Figure 22. Drawing “ideal” data achieved from sensors.

Data slices from sensor units are shown as blue dashed lines on original surface.

Drawing of noised data from sensor with random sensitivity.

```

figure2 = figure

```

```

surf(xx,yy,h,'facealpha',0.0)
for i=1:1:8
plot3(x,yy(dX(i),:),sliceXa(i,:), '-r')
hold on
end

for i=1:1:8
plot3(xx(:,dY(i)),y,sliceYa(i,:), '-r')
end

shading interp
axis tight
xlabel('x');
ylabel('y');
zlabel('intensity')

```

Result is shown on the following figure.

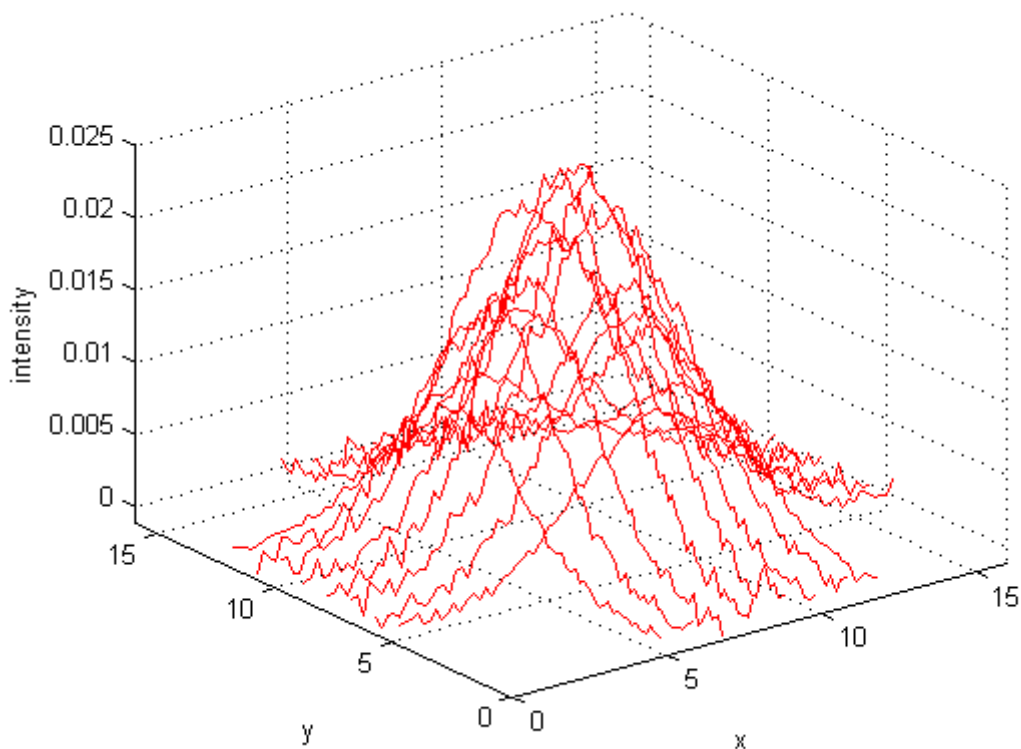


Figure 23. Drawing “real” (noised) data achieved from sensors with different sensitivity.

Integral evaluation of beam by one axis is achieved by summarizing all slices from same detector row to one.

```

%combining all slices by X axis in one
sliceAllX=zeros(1,81);
for i=1:1:8
    sliceAllX=sliceAllX+sliceXa(i,:);
end
%combining all slices by Y axis in one
sliceAllY=zeros(1,81);
for i=1:1:8
    sliceAllY=sliceAllY+sliceYa(i,:);
end

```

end

As a result we have one dimensional distribution dependant on only one axis (X or Y). Now we can calculate distribution parameters for appropriate coordinate (X independent from Y, and Y from X). Calculation of mathematical parameters of distribution achieved from sensor such as standard deviation and mean by axis can be achieved from integral evaluation of beam by each axis. Achieved parameters estimation (mean and standard deviation) for this one dimensional distribution is approximately the same for original distribution by this axis. But for two dimensional distribution is also necessary to achieve such important parameters as correlation coefficient by each axis. For correlation coefficient equal to 0 we have circle form of beam cross section and mean for each certain slice by axis is equal to one for the whole distribution by same axis. In other case it is not correct, mean for whole distribution and certain slice are different.

```
% normalizing
sliceAllXn=sliceAllX/sum(sliceAllX);
sliceAllYn=sliceAllY/sum(sliceAllY);
%calculation of mathematical parameters of distribution
[MuAX, SigmX]=statpar(sliceAllX); %from combined data by X axis
[MuAY, SigmY]=statpar(sliceAllY); %from combined data by Y axis
[MuAX1, SigmX1]=statpar(sliceX(1, :));%from first diode by X axis
[MuAY1, SigmY1]=statpar(sliceY(1, :));%from first diode by Y axis
```

Function `statpar` that was used to calculate mean and standard deviation from data is listed below.

```
function [ m,sigma ] = statpar( data )
summ=sum(data);
m=0;
for i=1:1:81
    m=m+(i-1)*data(i)/summ*0.2; %0.2 is discretization step
end
d=0;
for i=1:1:81
    d=d+data(i)/summ*((i-1)*0.2-m)*((i-1)*0.2-m);
end
sigma=sqrt(d);
end
```

Now we have asset of conditional probability distribution (slices from diodes) and those corresponding estimations and estimation of mean and standard deviation for the whole distribution. All those characteristics are linked with the following equations:

$$\begin{aligned} m[x/y] &= m_x + r_{xy} \sigma_x (y - m_y) / \sigma_y; & D[x/y] &= \sigma_x^2 (1 - r_{xy}^2); \\ m[y/x] &= m_y + r_{xy} \sigma_y (x - m_x) / \sigma_x; & D[y/x] &= \sigma_y^2 (1 - r_{xy}^2); \end{aligned} \quad (5)$$

where $m[x/y]$ - mean (X) for fixed (Y) i.e. mean for conditional distribution (X),
 $m[y/x]$ - mean (Y) for fixed (X) i.e. mean for conditional distribution (Y),
 m_x - mean (X) for the whole distribution; m_y - mean (Y) for the whole distribution,
 r_{xy} - correlation coefficient, σ_x - standard deviation by X axis for the whole distribution;
 σ_y - standard deviation by Y axis for the whole distribution; x - coordinate of diode by X axis in
Y-scanning row; y - coordinate of diode by Y axis in X-scanning row.

Following equation can be obtained as a result of transformation mentioned relations (5).

$$r_{xy} = \frac{m[x/y] - m_x}{y - m_y} \cdot \frac{\sigma_y}{\sigma_x}$$

$$[\sigma_y / \sigma_x] = [\sigma_x / \sigma_y]$$

Correlation coefficient have to be obtained as average for every combination X and Y diodes position in row and column, excluding those that lies mean to the mean to avoid dividing by zero. There are 64 possible combination but for simplification only 4 were used.

```
RtX1=(MuAX1-MuAX)/(posY(1)-MuAY)*SigmY1/SigmX1; %correlation
coeff.
RtY1=(MuAY1-MuAY)/(posX(1)-MuAX)*SigmX1/SigmY1; %correlation
coeff.
[MuAX2,SigmX2]=statpar(sliceX(8,:));%from last diode by X axis
[MuAY2,SigmY2]=statpar(sliceY(8,:));%from last diode by Y axis
RtX2=(MuAX2-MuAX)/(posX(8)-MuAY)*SigmY2/SigmX2;%correlation coeff.
RtY2=(MuAY2-MuAY)/(posX(8)-MuAX)*SigmX2/SigmY2;%correlation coeff.
%calculation of correlation coefficient as mean from 4 extreme
slices
RtXY=(RtX1+RtY1+RtX2+RtY2)/4;
```

Results of the script with different parameters are shown below.

Parameters (original / restored)	O	R	O	R	O	R	O	R	O	R
Mean X, (M _x / MuAX)	8	7.97	8	7.99	8	7.95	8	7.96	8	7.89
Mean Y, (M _y / MuAYX)	8	7.99	8	7.98	8	7.97	8	7.96	8	7.9
σ_x standard deviation X, (S _x / SigmX)	2.55	2.53	2.55	2.51	2.55	2.51	2.55	2.41	2.55	2.14
σ_y standard deviation Y,	2.55	2.53	2.55	2.55	2.55	2.48	2.55	2.41	2.55	2.19

(Sy / SigmY)										
Correlation coefficient, (Rxy / RtXY)	0.0	-8.36e-04	-0.1	-0.099	-0.2	-0.2	-0.5	-0.51	-0.8	-0.82

As can be seen from achieved results script can restore information adequately. It stands to mention that restoring algorithm is quite simple and can perform the task without information about certain sensitivity of each sensor. According to result calculation error increases as increases distance from demand parameters of distribution, but give enough information to correct beam parameters in right way.

Important conclusion: *all calculation deal with normalized conditional distributions, so there is no reason to make diodes sensitivity calibration.*

It is also possible to make calculations based on this algorithm to determine relative sensitivity of each sensor if direct data draw will be necessary to implement.

Interpolation algorithm

As soon as we achieved parameters of distribution and its slices by each axis we can now reconstruct spatial distribution of charged particles in beam more closely to real one. Notice that it has no practical meaning but if necessary it can be done the same way. (Reconstruction of intermediate points of distribution those were not scanned directly by detectors is out of scope of the task but can be described if such functionality will be requested later.)

Lets treat $f'(x/y_n)$ as normalized slice achieved from n sensitive unit of X detector part; $f''(x/y_n)$ - is the same slice scaled to real size.

We have n slices $f'(x/y_n)$ and n slice $f'(y/x_n)$ so we have $2n$ slices.

$f''(x/y_n)$ can be achieved by the following equation:

$$n(x/y_n)''_i = n(x/y_n)'_i \cdot \frac{\int_0^\infty \int_0^\infty \frac{1}{2\pi\sigma_x\sigma_y\sqrt{1-r_{xy}^2}} e^{-\frac{1}{2(1-r_{xy}^2)}\left[\frac{(x-m_x)^2}{\sigma_x^2} - \frac{2r_{xy}(x-m_x)(y_n-m_y)}{\sigma_x\sigma_y} + \frac{(y_n-m_y)^2}{\sigma_y^2}\right]} dx dy}{\sum_0^i n(x/y_n)_i}$$

where:

$n(x/y_n)'_i$ – i -value of discrete function $f'(x/y_n)$ ($f'(x/y_n)$ is represented as amount of discrete values);

$n(x/y_n)''_i$ – i -value of discrete function $f''(x/y_n)$ in right scale size;

i – index of current element from n ;

m_x - estimation of mean by X axis;

m_y - estimation of mean by Y axis;

r_{xy} - estimation of correlation coefficient;

σ_x - estimation of standard deviation by X axis;

σ_y - estimation of standard deviation by Y axis.

And $f''(y/x_n)$ can be achieved by the following equation:

$$n(y/x_n)_i'' = n(y/x_n)_i' \cdot \frac{\int_0^\infty \int_0^\infty \frac{1}{2\pi\sigma_x\sigma_y\sqrt{1-r_{xy}^2}} e^{-\frac{1}{2(1-r_{xy}^2)} \left[\frac{(x_n-m_x)^2}{\sigma_x^2} - \frac{2r_{xy}(x_n-m_x)(y-m_y)}{\sigma_x\sigma_y} + \frac{(y-m_y)^2}{\sigma_y^2} \right]} dx dy}{\sum_0^i n(y/x_n)_i}$$

where:

$n(y/x_n)_i'$ – i-value of discrete function $f'(y/x_n)$ ($f'(y/x_n)$ is represented as amount of discrete values);

$n(y/x_n)_i''$ – i-value of discrete function $f''(y/x_n)$ in right scale size;

i – index of current element from n ;

m_x - estimation of mean by X axis;

m_y - estimation of mean by Y axis;

r_{xy} - estimation of correlation coefficient;

σ_x - estimation of standard deviation by X axis;

σ_y - estimation of standard deviation by Y axis.

Now we have 8 n on n greed from beam distribution envelope curves, it is not very useful for draw interpretation so we can full fill gaps between x_n and x_{n+1} (and y_n and y_{n+1}) curves by using non-linear interpolation. It can be achieved by the following: for each $x_n < x_t < x_{n+1}$

$$f'''(y/x_t) = f'''(y/x_n) \frac{(f'(y/x_{n+1}) - f'(y/x_n))(x_{n+1} - x_t)}{x_{n+1} - x_n}$$

As result linear interpolated function was obtained $f'''(y/x_t)$. At the next step non-linear interpolated function can be found.

$$f''''(y/x_t) = f''''(y/x_t) \cdot \frac{\int_0^\infty \int_0^\infty \frac{1}{2\pi\sigma_x\sigma_y\sqrt{1-r_{xy}^2}} e^{-\frac{1}{2(1-r_{xy}^2)} \left[\frac{(x_t-m_x)^2}{\sigma_x^2} - \frac{2r_{xy}(x_t-m_x)(y-m_y)}{\sigma_x\sigma_y} + \frac{(y-m_y)^2}{\sigma_y^2} \right]} dx dy}{\sum_0^n f''''(x_t/y_t)}$$

Working cycle algorithm

At start up on control input of both switches comes logical one, that results in discharge of storage capacitors and connecting of detector to the ground. Then checked if detectors are in “parking zone” (starting area out of working area of irradiation) or not by checking zero-position detectors located at motors. If detectors are not in “parking zone” translation of X-scanning detector switches on firstly and then Y-scanning detector. After all these steps device is considered to be in starting position.

By signal from PC motor of X-axis switches on and detector moves at the first position of irradiation working area. At this moment temporary array with size equal by number of sensors in detector. All data in array is filled with zeros. At this point first measurement is achieved. Further routine depends on used mode.

In case of synchronious mode MCU waits for signal about beam start and then turn off switch 1 by applying logical “0” to its controlling input. Charge of storage capacitor with current from detectors starts at this moment. After 1 μ s switch 2 is turned off and switch 1 with several micro seconds delay turned on. Delay when both switches are off is necessary to avoid steady leakage current trough switches in duration of transient processes.

When second pulse from synchronization channel arrives switch1 turns off and switch 2 with 1 μ s delay turns off. In this condition storage capacitors are in charge keep mode. Then memory multiplexor of reading channel selection gets code of zero channel and embedded ADC of MCU gets voltage from first channel. At this stage cycle of AD conversions starts and all other MCU routine interrupts until end of the process. It helps to decrease influence of noises from CU of MCU on accuracy of ADC processes.

Digital code obtained summarized with first element in temporary storage array (that has zeros at the start). Then multiplexor of reading channel selection gets code from second channel and ADC of voltage from next capacitor takes places and after that digital code obtained summarizes with next array element.

Cycle repeats several times until all channels have been read (8/16). After that as full cycle has been completed, switches 1 and 2 are turned off starting process of charge of storage capacitors.

Then MCU waits next synchronization pulse and all routine repeats again. In the meanwhile in temporary storage array cumulates summary of measures from each channel. It helps to avoid errors related to imbecility of beam fluctuation from pulse to pulse.

Other possible scenario of synchronous mode is ADC of voltage on each storage capacitor doesn't take place at each cycle and switch 2 remains off until it gets next synchronization pulse of beam start and start of new cycle of measurements accordingly. Summarizing of charge from pulse to pulse takes places at storage capacitors directly.

Difference at asynchronous mode is that switch 1 turns off and switch 2 turns on in time without direct relation to beam pulses and remains at those condition for several certain beam pulses. Number of pulses is selected as parameter on PC by operator. Disadvantage of this mode is possible charge leakages in interval between pulses because of switch 2 that remains closed all the time during the process. Is that disadvantage sufficient or not can be explored experimentally by comparison of results in 3 possible modes.

Cycle repeats selected number of times for the same position of detector. Number of measurements at each point selected by PC program as a parameter. After selected number of repeats all temporary storage array sent to PC via USB. Transmission format: coordinate of detector position (1 byte) then array (2 bytes for each element). Then translation movement of detector part ob one step takes place and cycle of measure repeats for next point. Number of points (number of micro steps in range of axis X) is selected as parameter on PC. After all steps and measures by X axis have been done detector moves to "parking zone".

Then all motioned routine repeats for Y-scanning detector. It is necessary that while measurements by one axis takes place, detector of another axis was at "parking zone". It helps to avoid mechanical collisions and influences of detectors at each other when both detectors (X and Y) are connected parallel.

MCU program is possible to perform several secondary functions:

1. Performing measuring cycle in parking zones X and Y as with beam as without beam to measure basement of galvanic leakages of diodes.
2. Setting of both detectors independently in the middle of the window of device for checking position of device relatively to the beam with calibration crosses.
3. Setting detectors in certainly selected position.
4. Testing mode without beam

Interface of PC program

Main window of PC program for developed device is shown at the following figure.

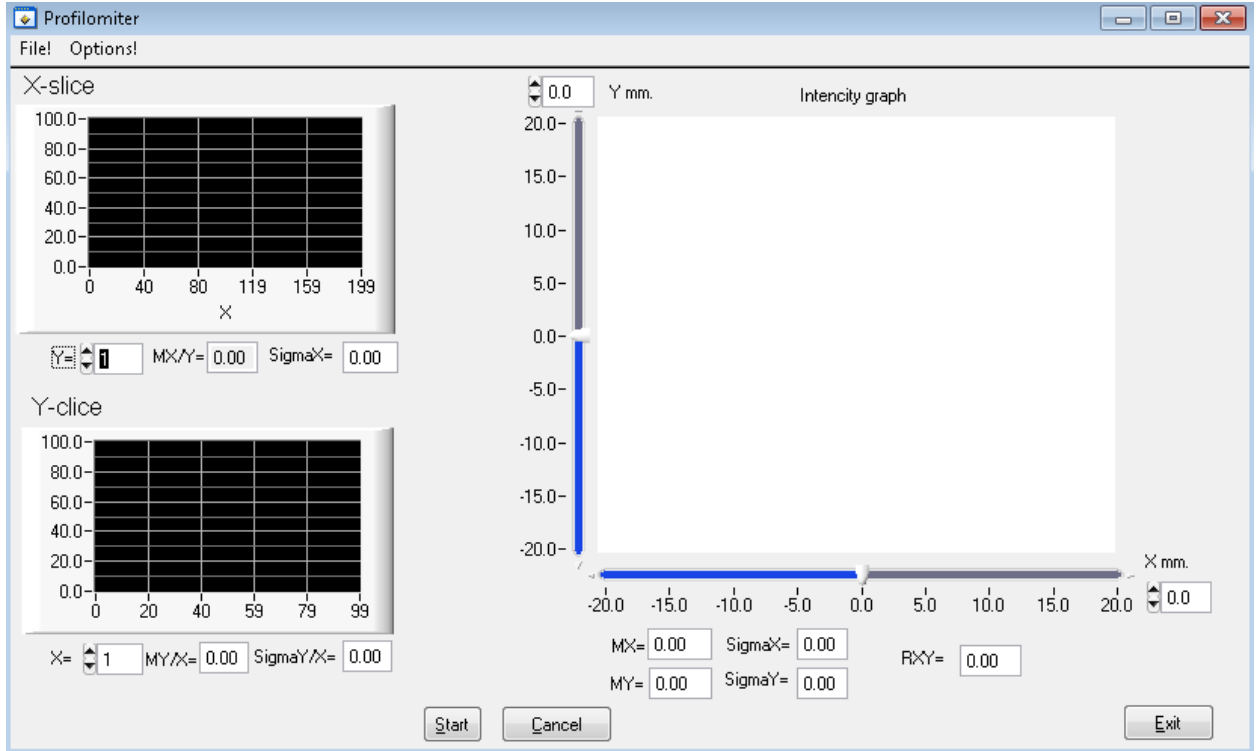


Figure 24. Interface of PC program.

Program is able to draw certain slices for both X-axis and Y-axis measurements and reconstruct overall distribution where intensity is shown with color changes. Parameters of distribution can be shown in according output windows in the end of scanning process.

Program is possible to switch manually between 3 different modes: synchronous, synchronous without ADC on each pulse and asynchronous.

It is also possible to execute 4 mentioned secondary functions of device from menu.

Components used

CAD model of device is shown at the following device. For simplicity wires and connections are not shown.

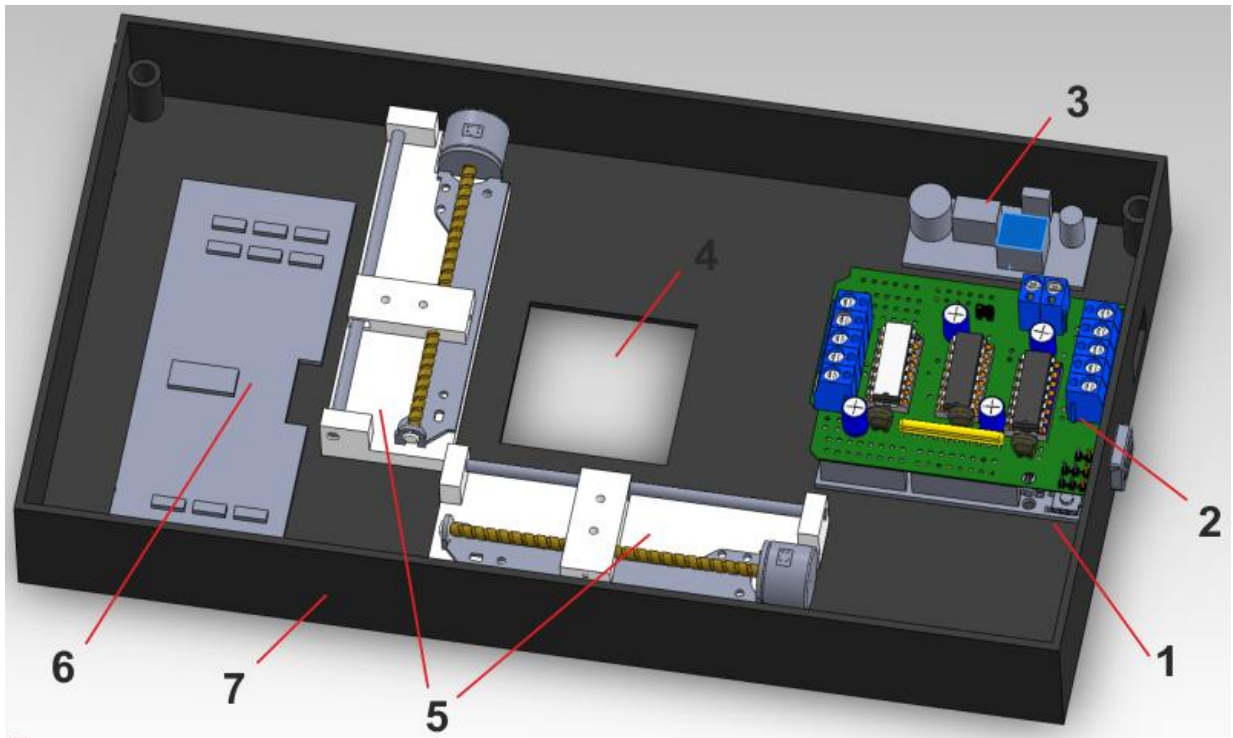


Figure 25. Device CAD model.

- 1 – MCU board Arduino Uno; 2 – Arduino motor shield v1.2
- 3 - Step down voltage convertor LM2596; 4 – window of working area;
- 5 – stepper motors with screw-shaft rotor; 6 - PCB with switches and memory multiplexor;
- 7 – device container without cover

All components will be described in details in following chapters. Schemes of electrical connections can be seen at the appendix (version for Arduino Nano is presented).

Arduino Uno

Arduino Uno was selected as main MCU used in this project. As can be seen from the characteristics described in details below it can operate on voltage level of 20V. It is very useful for the purpose of this task because same voltage can be used as blocking voltage for sensitive units. Arduino Uno also has enough digital and anal I/O to perform task of this work. Handy shield for motor control can be connected directly to Arduino Uno connectors.



Figure 26. Top and bottom side of arduino Uno (image taken from arduino.cc).

More detailed information is given below.

Overview

The Arduino Uno is a microcontroller board based on the ATmega328 (datasheet). It has 14 digital input/output pins (of which 6 can be used as PWM outputs), 6 analog inputs, a 16 MHz ceramic resonator, a USB connection, a power jack, an ICSP header, and a reset button. It contains everything needed to support the microcontroller; simply connect it to a computer with a USB cable or power it with a AC-to-DC adapter or battery to get started.

"Uno" means one in Italian and is named to mark the upcoming release of Arduino 1.0. The Uno and version 1.0 will be the reference versions of Arduino, moving forward. The Uno is the latest in a series of USB Arduino boards, and the reference model for the Arduino platform.

Summary

Microcontroller ATmega328

Operating Voltage 5V

Input Voltage (recommended) 7-12V

Input Voltage (limits) 6-20V

Digital I/O Pins 14 (of which 6 provide PWM output)

Analog Input Pins 6

DC Current per I/O Pin 40 mA

DC Current for 3.3V Pin 50 mA

Flash Memory 32 KB (ATmega328) of which 0.5 KB used by bootloader

SRAM 2 KB (ATmega328)

EEPROM 1 KB (ATmega328)

Clock Speed 16 MHz

Length 68.6 mm

Width 53.4 mm

Weight 25 g

Schematic & Reference Design

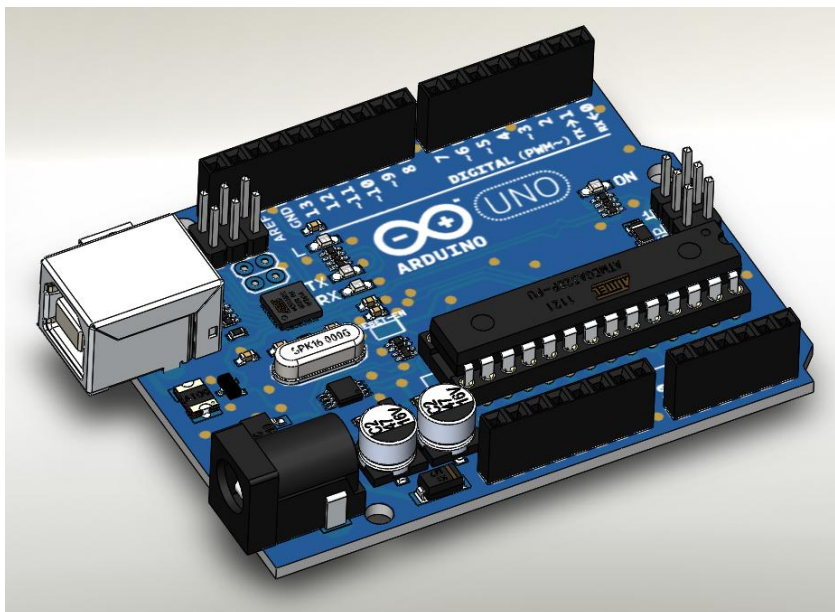


Figure 27. Arduino Uno CAD model (taken from grabcad.com)

Power

The Arduino Uno can be powered via the USB connection or with an external power supply. The power source is selected automatically.

External (non-USB) power can come either from an AC-to-DC adapter (wall-wart) or battery. The adapter can be connected by plugging a 2.1mm center-positive plug into the board's power jack. Leads from a battery can be inserted in the Gnd and Vin pin headers of the POWER connector.

The board can operate on an external supply of 6 to 20 volts. If supplied with less than 7V, however, the 5V pin may supply less than five volts and the board may be unstable. If using more than 12V, the voltage regulator may overheat and damage the board. The recommended range is 7 to 12 volts.

The power pins are as follows:

VIN. The input voltage to the Arduino board when it's using an external power source (as opposed to 5 volts from the USB connection or other regulated power source). You can supply voltage through this pin, or, if supplying voltage via the power jack, access it through this pin.

5V. This pin outputs a regulated 5V from the regulator on the board. The board can be supplied with power either from the DC power jack (7 - 12V), the USB connector (5V), or the VIN pin of the board (7-12V). Supplying voltage via the 5V or 3.3V pins bypasses the regulator, and can damage your board. We don't advise it.

3V3. A 3.3 volt supply generated by the on-board regulator. Maximum current draw is 50 mA.

GND. Ground pins.

IOREF. This pin on the Arduino board provides the voltage reference with which the microcontroller operates. A properly configured shield can read the IOREF pin voltage and select the appropriate power source or enable voltage translators on the outputs for working with the 5V or 3.3V.

Memory

The ATmega328 has 32 KB (with 0.5 KB used for the bootloader). It also has 2 KB of SRAM and 1 KB of EEPROM (which can be read and written with the EEPROM library).

Input and Output

Each of the 14 digital pins on the Uno can be used as an input or output. They operate at 5 volts. Each pin can provide or receive a maximum of 40 mA and has an internal pull-up resistor (disconnected by default) of 20-50 kOhms. In addition, some pins have specialized functions:

Serial: 0 (RX) and 1 (TX). Used to receive (RX) and transmit (TX) TTL serial data. These pins are connected to the corresponding pins of the ATmega8U2 USB-to-TTL Serial chip.

External Interrupts: 2 and 3. These pins can be configured to trigger an interrupt on a low value, a rising or falling edge, or a change in value. See the `attachInterrupt()` function for details.

PWM: 3, 5, 6, 9, 10, and 11. Provide 8-bit PWM output with the `analogWrite()` function.

SPI: 10 (SS), 11 (MOSI), 12 (MISO), 13 (SCK). These pins support SPI communication using the SPI library.

LED: 13. There is a built-in LED connected to digital pin 13. When the pin is HIGH value, the LED is on, when the pin is LOW, it's off.

The Uno has 6 analog inputs, labeled A0 through A5, each of which provide 10 bits of resolution (i.e. 1024 different values). By default they measure from ground to 5 volts, though it is possible to change the upper end of their range using the AREF pin and the `analogReference()` function. Additionally, some pins have specialized functionality:

TWI: A4 or SDA pin and A5 or SCL pin. Support TWI communication using the Wire library.

There are a couple of other pins on the board:

AREF. Reference voltage for the analog inputs. Used with `analogReference()`.

Reset. Bring this line LOW to reset the microcontroller. Typically used to add a reset button to shields which block the one on the board.

See also the mapping between Arduino pins and ATmega328 ports. The mapping for the Atmega8, 168, and 328 is identical.

Communication

The Arduino Uno has a number of facilities for communicating with a computer, another Arduino, or other microcontrollers. The ATmega328 provides UART TTL (5V) serial communication, which is available on digital pins 0 (RX) and 1 (TX). An

ATmega16U2 on the board channels this serial communication over USB and appears as a virtual com port to software on the computer. The '16U2 firmware uses the standard USB COM drivers, and no external driver is needed. However, on Windows, a .inf file is required. The Arduino software includes a serial monitor which allows simple textual data to be sent to and from the Arduino board. The RX and TX LEDs on the board will flash when data is being transmitted via the USB-to-serial chip and USB connection to the computer (but not for serial communication on pins 0 and 1).

A SoftwareSerial library allows for serial communication on any of the Uno's digital pins.

The ATmega328 also supports I2C (TWI) and SPI communication. The Arduino software includes a Wire library to simplify use of the I2C bus; see the documentation for details. For SPI communication, use the SPI library.

Programming

The Arduino Uno can be programmed with the Arduino software (download).

The ATmega328 on the Arduino Uno comes preburned with a bootloader that allows to upload new code to it without the use of an external hardware programmer. It communicates using the original STK500 protocol.

Automatic (Software) Reset

Rather than requiring a physical press of the reset button before an upload, the Arduino Uno is designed in a way that allows it to be reset by software running on a connected computer. One of the hardware flow control lines (DTR) of the ATmega8U2/16U2 is connected to the reset line of the ATmega328 via a 100 nanofarad capacitor. When this line is asserted (taken low), the reset line drops long enough to reset the chip. The Arduino software uses this capability to allow you to upload code by simply pressing the upload button in the Arduino environment. This means that the bootloader can have a shorter timeout, as the lowering of DTR can be well-coordinated with the start of the upload.

This setup has other implications. When the Uno is connected to either a computer running Mac OS X or Linux, it resets each time a connection is made to it from software (via USB). For the following half-second or so, the bootloader is running on the Uno. While it is programmed to ignore malformed data (i.e. anything besides an upload of new code), it will intercept the first few bytes of data sent to the board after a connection is

opened. If a sketch running on the board receives one-time configuration or other data when it first starts, make sure that the software with which it communicates waits a second after opening the connection and before sending this data.

The Uno contains a trace that can be cut to disable the auto-reset. The pads on either side of the trace can be soldered together to re-enable it. It's labeled "RESET-EN". You may also be able to disable the auto-reset by connecting a 110 ohm resistor from 5V to the reset line; see this forum thread for details.

USB Overcurrent Protection

The Arduino Uno has a resettable polyfuse that protects your computer's USB ports from shorts and overcurrent. Although most computers provide their own internal protection, the fuse provides an extra layer of protection. If more than 500 mA is applied to the USB port, the fuse will automatically break the connection until the short or overload is removed.

Physical Characteristics

The maximum length and width of the Uno PCB are 2.7 and 2.1 inches respectively, with the USB connector and power jack extending beyond the former dimension. Four screw holes allow the board to be attached to a surface or case. Note that the distance between digital pins 7 and 8 is 160 mil (0.16"), not an even multiple of the 100 mil spacing of the other pins.

Arduino motor shield v1.2

Shield is used in combination with Arduino Uno because it was designed specially for it. Shield allows to control 2 bipolar 3 wire steppers those are used in the task.

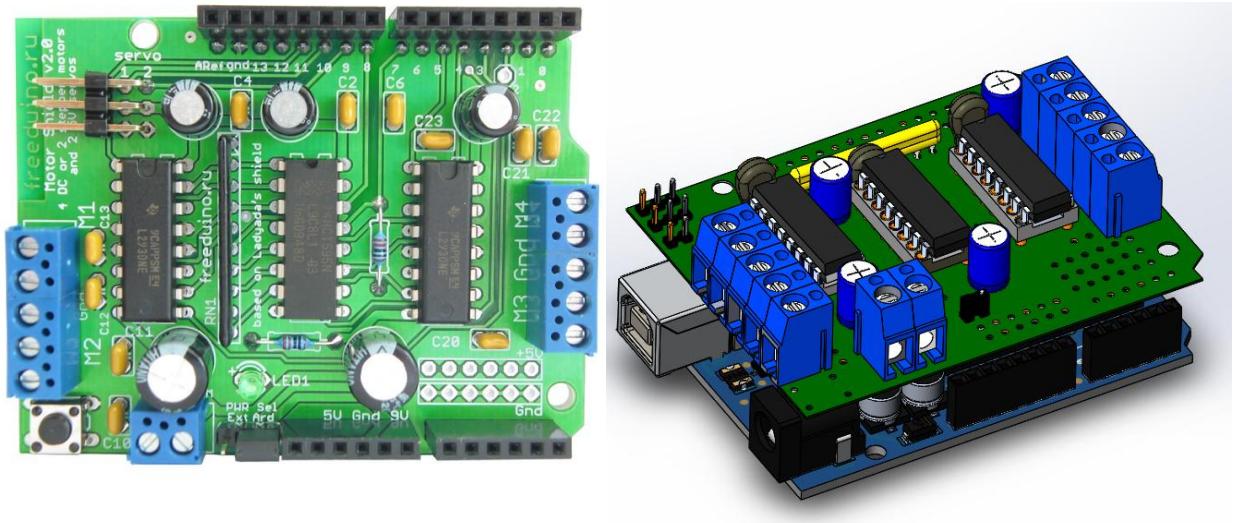


Figure 28. Arduino compatible motor shield v1.2 (top view and CAD model with Arduino Uno connected, model taken from grabcad.com, image taken from arduino.cc).

Detailed description to the motor shield is given below:

Arduino motor shield is a PCB that is able to power many simple to medium-complexity projects.

2 connections for 5V servos connected to the Arduino's high-resolution dedicated timer.

4 H-Bridges: L293D chipset provides 0.6A per bridge (1.2A peak) with thermal shutdown protection, internal kickback protection diodes. Can run motors on 4.5VDC to 25VDC.

Up to 4 bi-directional DC motors with individual 8-bit speed selection (so, about 0.5% resolution)

Up to 2 stepper motors (unipolar or bipolar) with single coil, double coil or interleaved stepping.

Pull down resistors keep motors disabled during power-up.

Big terminal block connectors to easily hook up wires (18-26AWG) and power.

Arduino reset button brought up top.

2-pin terminal block and jumper to connect external power, for separate logic/motor supplies.

Using Stepper motors

Stepper motors are great for (semi-)precise control, perfect for many robot and CNC projects. This motor shield supports up to 2 stepper motors. The library works identically for bi-polar and uni-polar motors

For unipolar motors: to connect up the stepper it is necessary to figure out which pins connected to which coil, and which pins are the center taps. If its a 5-wire motor then there will be 1 that is the center tap for both coils. The center taps should both be connected together to the GND terminal on the motor shield output block. Then coil 1 should connect to one motor port (M1 or M3) and coil 2 should connect to the other motor port (M2 or M4).

For bipolar motors: its just like unipolar motors except there is no 5th wire to connect to ground. The code is exactly the same.

Stepper motors can be easily controlled using available library for arduino and this motor shield. It makes possible to control motors in several different modes: single coil step, double coil step, interleave coil step , microstep steps.

Shield uses as driver 2 micropships L293D with H-Bridges.

L293D motor driver

L293d motor driver is used as part of motor shield. Its inner schematics with H-Bridges allows to operate bipolar stepper motors those are used in this project. L293D inner construction is shown at the following figure.

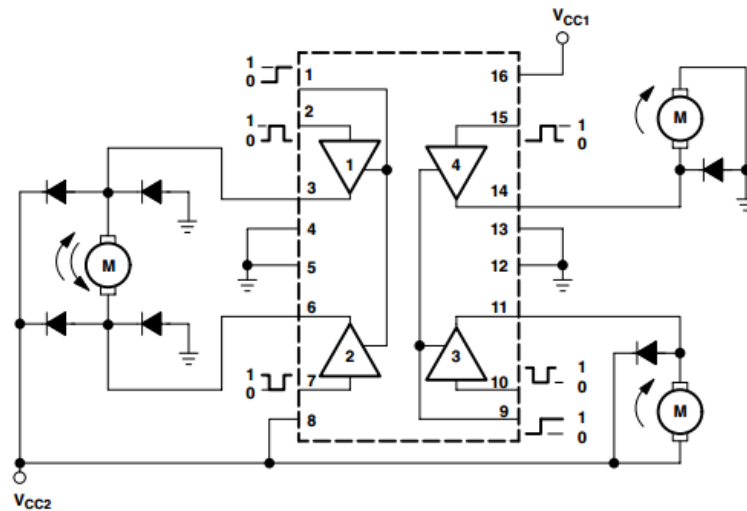


Figure 29. Scheme of L293D driver.

Main features of this chip are described below:

Features

Products Now From Texas Instruments

Wide Supply-Voltage Range: 4.5 V to 36 V

Separate Input-Logic Supply

Internal ESD Protection

Thermal Shutdown

High-Noise-Immunity Inputs

Output Current 600mA Per Channel

Peak Output Current 1.2 A Per Channel

Output Clamp Diodes for Inductive

Transient Suppression

Description

The L293 and L293D are quadruple high-current half-H drivers. The L293 is designed to provide bidirectional drive currents of up to 1 A at voltages from 4.5 V to 36 V. The L293D is designed to provide bidirectional drive currents of up to 600-mA at voltages from 4.5 V to 36 V. Both devices are designed to drive inductive loads such as relays, solenoids, dc and bipolar stepping motors, as well as other high-current/high-voltage loads in positive-supply applications.

All inputs are TTL compatible. Each output is a complete totem-pole drive circuit, with a Darlington transistor sink and a pseudo Darlington source. Drivers are enabled in pairs, with drivers 1 and 2 enabled by 1,2EN and drivers 3 and 4 enabled by 3,4EN. When an enable input is high, the associated drivers are enabled, and their outputs are active and in phase with their inputs. When the enable input is low, those drivers are disabled, and their outputs are off and in the high-impedance state. With the proper data inputs, each pair of drivers forms a full-H (or bridge) reversible drive suitable for solenoid or motor applications.

PCB with switches and memory multiplexor

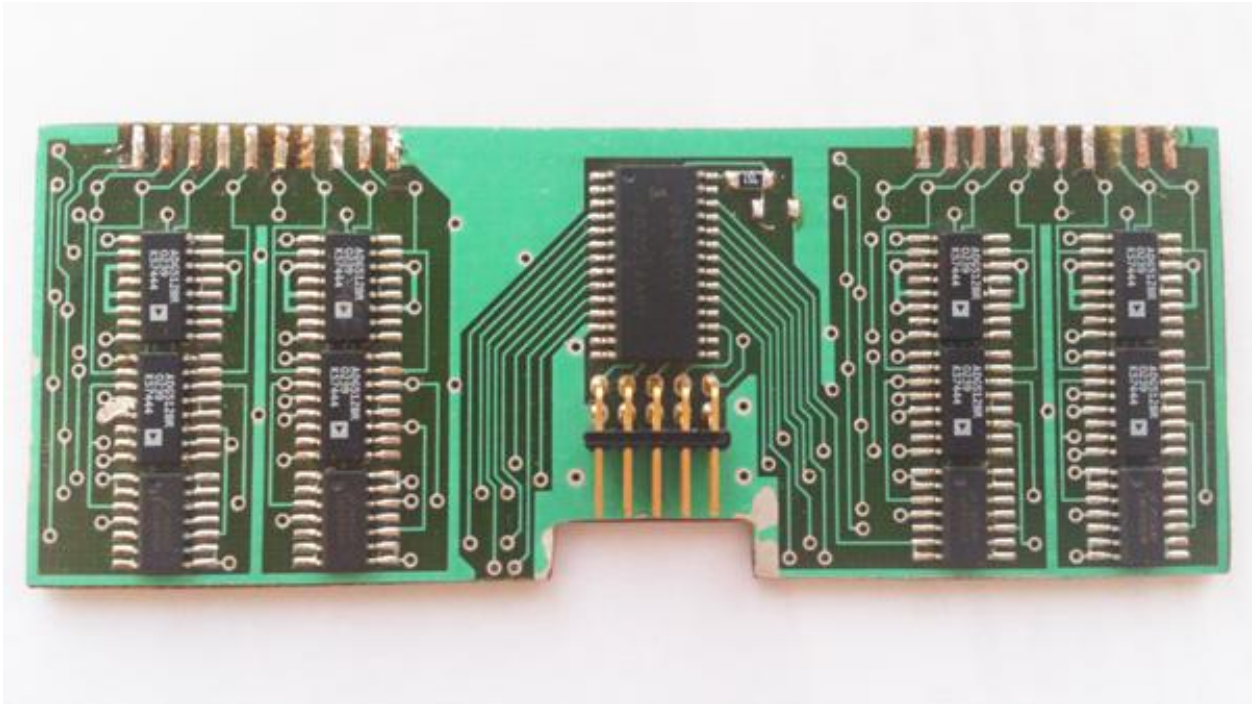


Figure 30. PCB with analog switches and 16-channel memory multiplexor.

Schematic of S&S part was changed in the last version of device (that doesn't effect working cycle described above). PCB on above figure has 8 channels for X-axis and 8 channels for Y axis. Each channel have operational amplifier (LMC660) with amplifying coefficient equal to 1 to prevent self discharge of capacitors. PCB also includes 16-channel multiplexor DG406. Multiplexor was used to read information from 16 sensor units. I take to account that motor shield uses 11 from 14 available digital pins to control motors there are only 6 analog channels and 3 digitals are left. 6 analog channels can be used as digital so in total there are 9 channels. 2 channels are used to read information from 2 null position detectors, and 2 to control analog switches. As soon as multiplexor is 16 channel it is necessary to have 4 channels to operate it. So there is only 1 analog channel left for actual information.

Storage capacitors are soldered to other side of PCB. Capacitors nominal of 2nf is taken to allow high sensitivity and not to exceed level of 5V that can be read by MCU ADC. More accurate nominal of capacitors will be selected as result of experiments.

Step down voltage convertor LM2596

Reduces input voltage level from 20V to 6V. Lowered voltage level of 6V is used to supply stepper motors. 20V level is used to supply Arduino Uno board that already has embedded LDO regulator to 5V. This voltage level is used to supply MCU.



Figure 31. Step down voltage convertor

Main features and detailed description of this component:

Features

3.3V, 5V, 12V, and Adjustable Output Versions

Adjustable Version Output Voltage Range, 1.2V to 37V $\pm 4\%$ Max Over Line and Load Conditions

Available in TO-220 and TO-263 Packages

Input Voltage Range Up to 40V

Requires Only 4 External Components

Excellent Line and Load Regulation Specifications

150 kHz Fixed Frequency Internal Oscillator

TTL Shutdown Capability

Low Power Standby Mode, I_q Typically 80 μA

High Efficiency

Uses Readily Available Standard Inductors

Thermal Shutdown and Current Limit Protection

Description

The LM2596 series of regulators are monolithic integrated circuits that provide all the active functions for a step-down (buck) switching regulator, capable of driving a 3A load with excellent line and load regulation. These devices are available in fixed output voltages of 3.3V, 5V, 12V, and an adjustable output version.

Requiring a minimum number of external components, these regulators are simple to use and include internal frequency compensation, and a fixed-frequency oscillator.

The LM2596 series operates at a switching frequency of 150 kHz thus allowing smaller sized filter components than what would be needed with lower frequency switching regulators. Available in a standard 5-lead TO-220 package with several different lead bend options, and a 5-lead TO-263 surface mount package.

A standard series of inductors are available from several different manufacturers optimized for use with the LM2596 series. This feature greatly simplifies the design of switch-mode power supplies.

Other features include an ensured $\pm 4\%$ tolerance on output voltage under specified input voltage and output load conditions, and $\pm 15\%$ on the oscillator frequency. External shutdown is included, featuring typically 80 μA standby current. Self protection features include a two stage frequency reducing current limit for the output switch and an over temperature shutdown for complete protection under fault conditions.

Schematic is shown below.

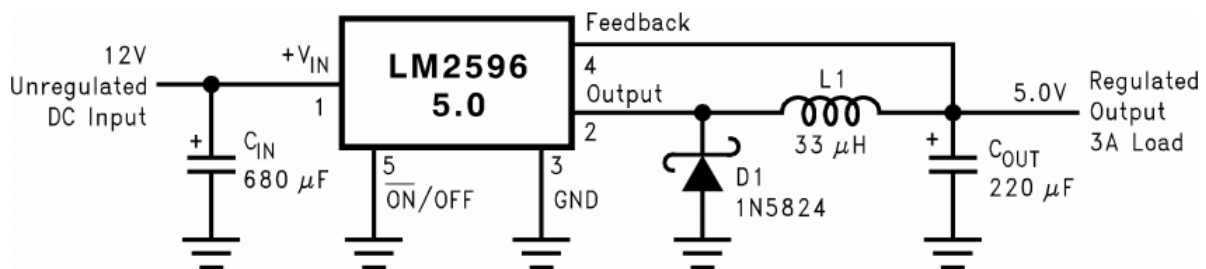


Figure 32. LM2595 Schematics

Conclusions

Developed device is quite flexible system and any modification can be added if necessary. Semiconductor detector was chosen as sensitive unit for this task because it has quite high spatial and time resolution that was approved by several publications and experiments. As soon as actual spatial configuration of crystal in semiconductor detector (as with its interoperability with radiation) is not provided by manufacturer the idea of project was to use wide-spread and so far easily available on market semiconductor (was used MMSD4148 diode in sod123 package) and configure parameters of the system experimentally for this selected model. Choice of cheap sensor is also rationally motivated because sensitive unit in condition of frequent usage will suffer degradation and as result sensitivity loss. For this purpose was designed handy fixture for detector part. It allows easily replacement if detector degraded critically or if detector with different modification is planned to use.

Developed working algorithm is able to reconstruct beam spatial distribution by scanning beam profile with multichannel detector and natural sensitivity scattering of sensitive units. As soon as actual numerical characteristic of beam overall intensity is known (with adequately accuracy $\pm 5\%$) as nominal value, task of scanning process come down to determining relative spatial distribution of particles in the beam. Performed mathematical modeling also shows that usage of methods of mathematical statistics allows to ignore natural sensitivity scattering of sensor units in detector part as it doesn't make sufficient influence on the process of spatial distribution reconstruction.

Was performed electric circuit modeling of single sensor unit in several different modes. It demonstrates how measuring without direct synchronization with beam pulses can be performed and how flexibility of system sensitivity can be achieved by changing number of pulses read by single unit.

Developed mechanical part allows to perform demand minimal translation step and requirement of preventing unnecessary unit degradation by ability to move detector part out of beam influence.

Suggested configuration of detector part with 8 sensor units with distance of 1mm between each is not optimal for beam size of 6 on 6mm on half high. It is recommended to increase size between sensitive unit up to 1,5mm or number of units up to 16 for each axis. Number of sensor units can be increased easily by using benefits of sample and store block configuration with memory multiplexor on 16 channels.

Kokkuvõte

Väljatöötatud seade on võrdlemisi paindlik süsteem ja vajadusel saab sellele lisada erinevaid modifikatsioone. Pooljuhtdetektor valiti tundlikuks elemendiks, kuna see annab üsna kõrge ruumilise ja ajalise eraldusvõime. See on heaks kiidetud ka mitmetes publikatsioonides ja katsetes. Kuna pooljuhtdetektori kristalli tegelik ruumiline konfiguratsioon (ja radiatsiooni puutuv kasutatavus) ei olnud tootja poolt antud, siis tekkis idee kasutada laialt levinud ja seni kergesti hangitavat pooljuhti (MMSD4148 diood sod123 korpuses) ning seadistada süsteemi parameetrid hiljem sellele komponendile vastavaks. Valik odava anduri kasuks on samuti põhjendatud, kuna tiheda kasutamise käigus halveneb tundliku elemendi kvaliteet ning põhjustab tundlikkuse vähenemist. Sel põhjusel konstrueeriti ka mugav detektorelemendi kinnitus. See võimaldab kerget väljavahetamist, kui detektor on otsustavalt kahjustunud või kui plaanitakse kasutada ümber tehtud detektorit.

Väljatöötatud algoritm võimaldab prootonkiire ruumilist jaotust rekonstrueerida, skaneerides prootonkiirt mitmekanalilise detektoriga, mille tundlikel elementidel esineb loomulikke tundlikkuse kõrvalekaldeid.

Kohe, kui prootonkiire üldine intensiivsus-karakteristik on nominaalväärtusena numbriliselt teada (piisava täpsusega $\pm 5\%$), jääb üle kindlaks teha skaneerimise abil osakeste suhteline ruumiline jaotus prootonkiires. Matemaatiline modelleerimine näitas muuhulgas, et matemaatilise statistika meetodite kasutamine lubab ignoreerida detektoris asuvate andurelementide loomuliku tundlikkuse hajumist, kuna sel ei ole ruumilise jaotuse rekonstrueerimise juures piisavat mõju.

Ühe-elementilise üksuse elektriskeemi modelleerimine teostati mitmetes erinevates režiimides. Tulemus demonstreerib, kuidas on mõõtmise teostatav, ilma prootonkiire impulssidega otseselt sünkroniseerimata ja kuidas süsteemi paindlikkus tundlikkuse osas on saavutatav selliselt, et muudetakse ühe elemendi poolt loetavate impulsside arvu.

Väljatöötatud mehhaanika osa lubab teostada nõutavaid minimaalseid nihkeid ning liigutada detektori osa ära prootonkiire mõju eest, vältides sellega detektori mittevajalikkukahjustumist.

Väljapakutud detektori konfiguratsioon kasutab 8 andurelementi 1 mm sammuga, mis ei ole 6 mm korda 6 mm poole doosi puhul optimaalne. Soovitatav oleks elementide sammu suurendamine 1,5 mm-ni või suurendada andurelementide arvu igal teljel 16-ni. Andurelementide arvu saab kergesti suurendada, kui kasutada 16-kanalilist mälu multiplekserit ja hoide-võrdlus lülitust.

References

1. Tyurin, E.I., Simbirceva, L.P., Konnov, B.A. and others, Report: Theme 05.02.01 Develop new methods of irradiation using proton synchrocyclotron of Leningrad Institute of Nuclear Physics n.a. B.P.Kosntantinov for stereotoxic and neurosurgery purpose., UDC 615.849.5:589.125.4:615.8-089 Reg. №81011344, PNPI, 1985.
2. Seliverstov, D.M., Proton medical system in PNPI, PNPI.
3. Abrosimov, N.K., Karlin, D.L., Konnov, B.A., Lazarev, V.I., Melnikov, L.A., Rjabov, G.A., Seliverstov, D.M.. Proton therapy on synchrocyclotron of PNPI, PNPI.
4. Durante, M., Varentsov, D., Proton therapy and radiography project (PaNTERA), GSI Sciencific Report, 2011.
5. Shirokov, U.M., Udin, N.P., Nuclear Physics, M: Nauka, 1980.
6. Kjellberg, R.N., Hanamura, T., Davis, K.R., Lyons, S.Z., Adams, R.D., Bragg-peak proton-beam therapy for arteriovenous malformations of the brain., The new England Journ. of Medicine., 1983, v.309, N5.
7. Volchenkov, V.A., Rjabov, G.A., Program for calculation beam optics in spatial field of synchrocyclotron on 1GeV., PNPI, 1971.
8. Abrosimov, N.K., Volchenkov, V.A., Rjabov, G.A., PC-program for calculation beam primary and secondary particles using Monte-Carlo method (“Mezon”), PNPI, 1975.
9. Akimov, U.K., Kalinin, A.I., Kushniruk, A.I., Jungklaussen, H., Semiconductor detectors of nuclear particles and its application, M:Atomizdat, 1967.
10. Petuchkov, A.A., Semiconductor detectors of nuclear radiation in medicine and biology, M:Medicine, 1976.

11. Raju, M.R., Heavy particle studies with silicon detectors, *Radat. Res. Suppl.*, 7.43, 1976.
12. Raju, M.R., The use of miniature silicon diode as a radiation dose meter, *Phys. Med. Biol.*, 11: 371, 1966.
13. Raju, M.R., Lyman, J.T., Brustad, T., Tobias, C.A., Heavy-charged-particle-beams, in *Radiation Dosimetry*, Vol.3, Academic Press, 1969.
14. Karlin, D.L., Konnov, B.A., Kostachenko, V.I. and others. Comparative dosimetry of medical proton beams in JINR, JINR, 1982.
15. Report of Central X-Ray and Radiology Research Institute of USSR “Develop and test method to use proton beam of PNPI with energy 1GeV for treating pituitary tumor and diseases of central nervous system.”, UDC 615.849.5:616.8 + 616.432)., 1980.
16. Hardy, K.A, Mitchell, J.C., Allen, S.J., Measurements of depth-dose distribution in cylindrical phantom exposed to 20-Mev, 21MeV, 14MeV, 5MeV protons, *Rad. Pes.*, 1967. v37, p.272-278.
17. Baribaud, G., The 800 MeV measurement line of the CERN PS booster, *IEEE*, 1973.
18. Verentsov, D., “High-energy proton microscopy of radiobiology-relevant targets”, GSI Scientific Report , 2012.
19. Sivuhin, D.V., *Common course of physics, part 2: nuclear physics*, 1986.
20. Backhaus, M., Characterization of new hybrid pixel module concepts for the ATLAS Insertable B-Layer upgrade, JINST, 2012.

Appendix

PCB

Presented PCB were used in early version of device with Arduino Nano modification.

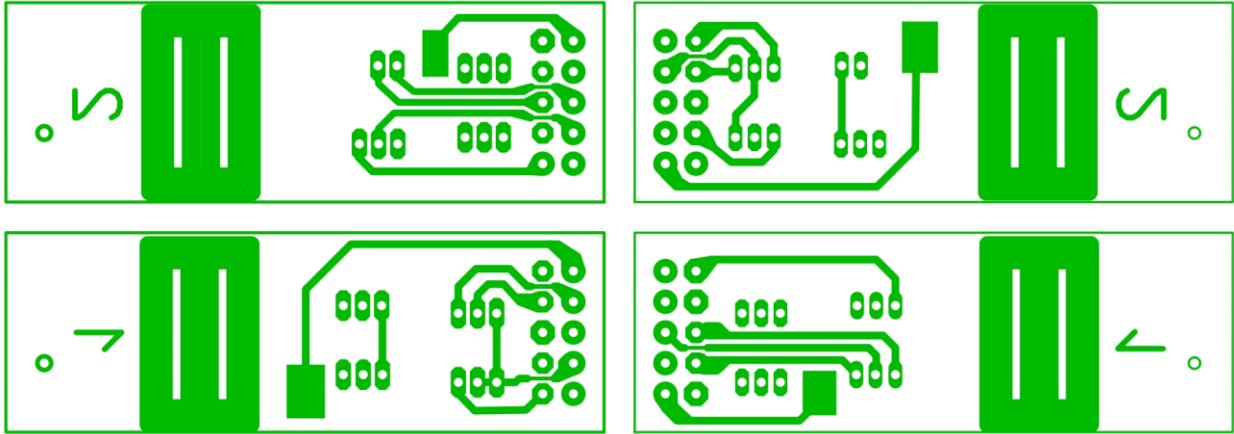


Figure 33. PCB for connection detector part and flexible flat cable



Figure 34. PCB for diodes (detector part)



Figure 34. Flexible flat cable

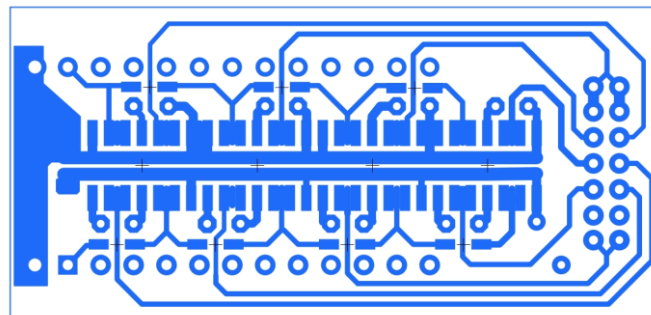


Figure 35. PCB for analog switches and storage capacitors

Photo

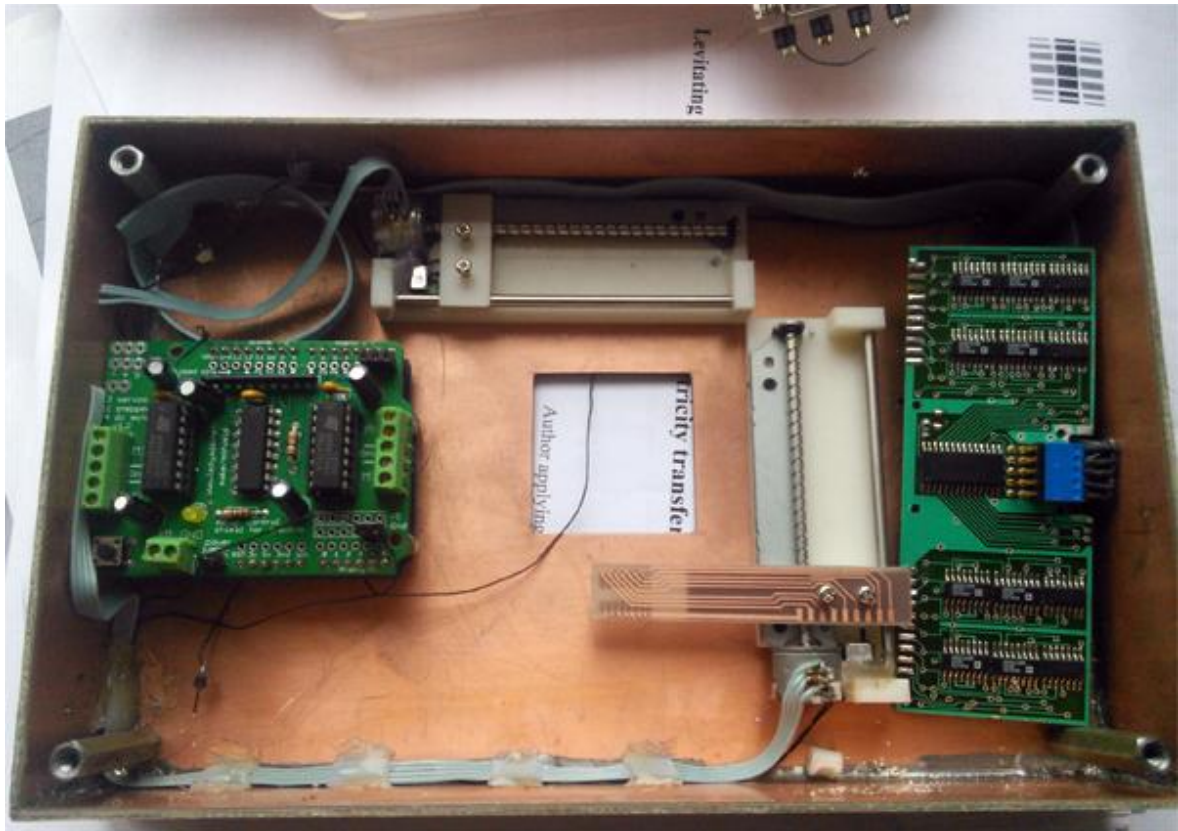
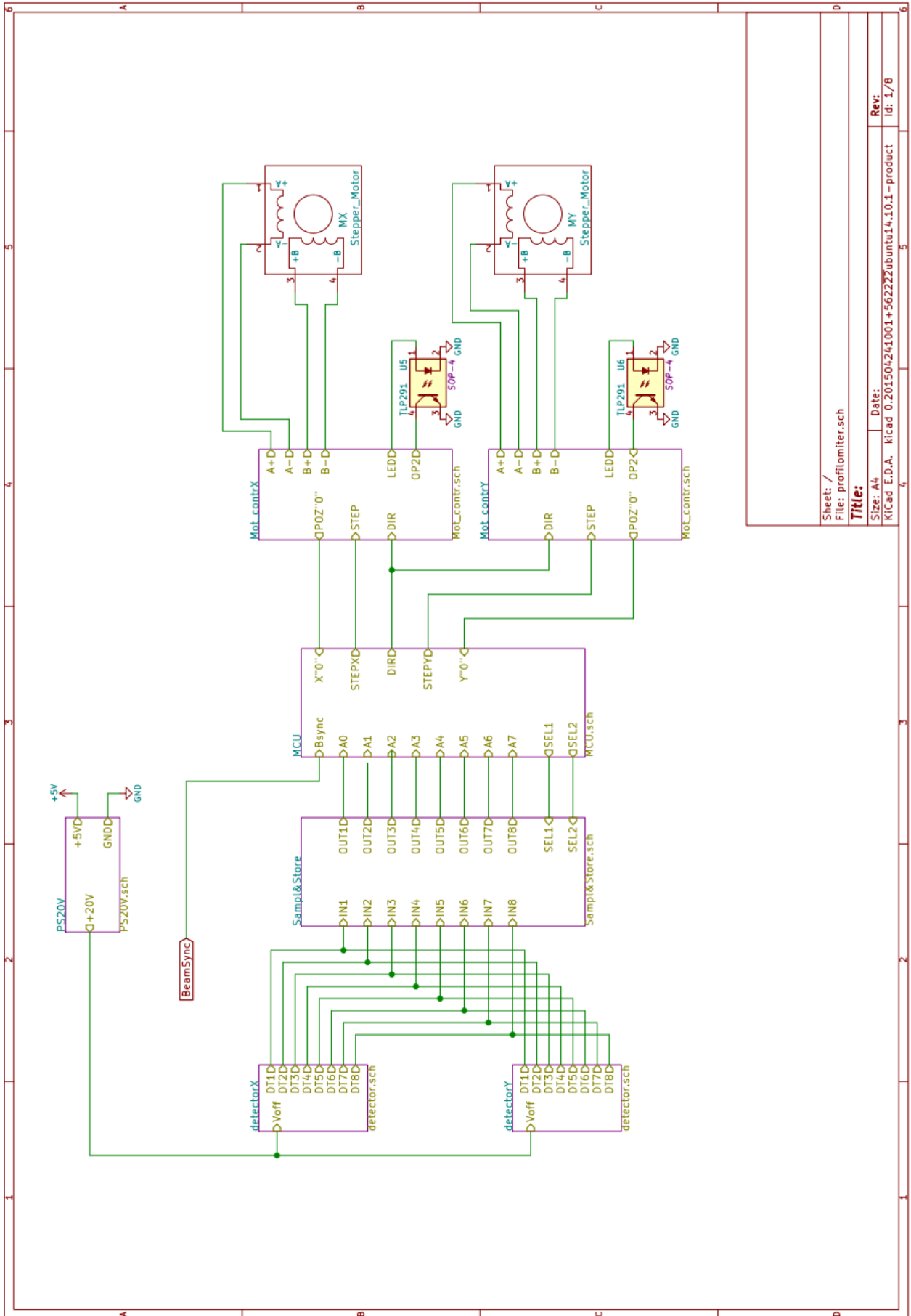
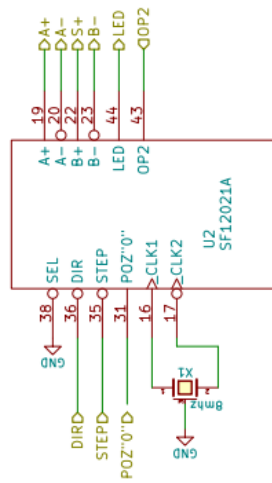


Figure 36. Device in assembly process

Schemes



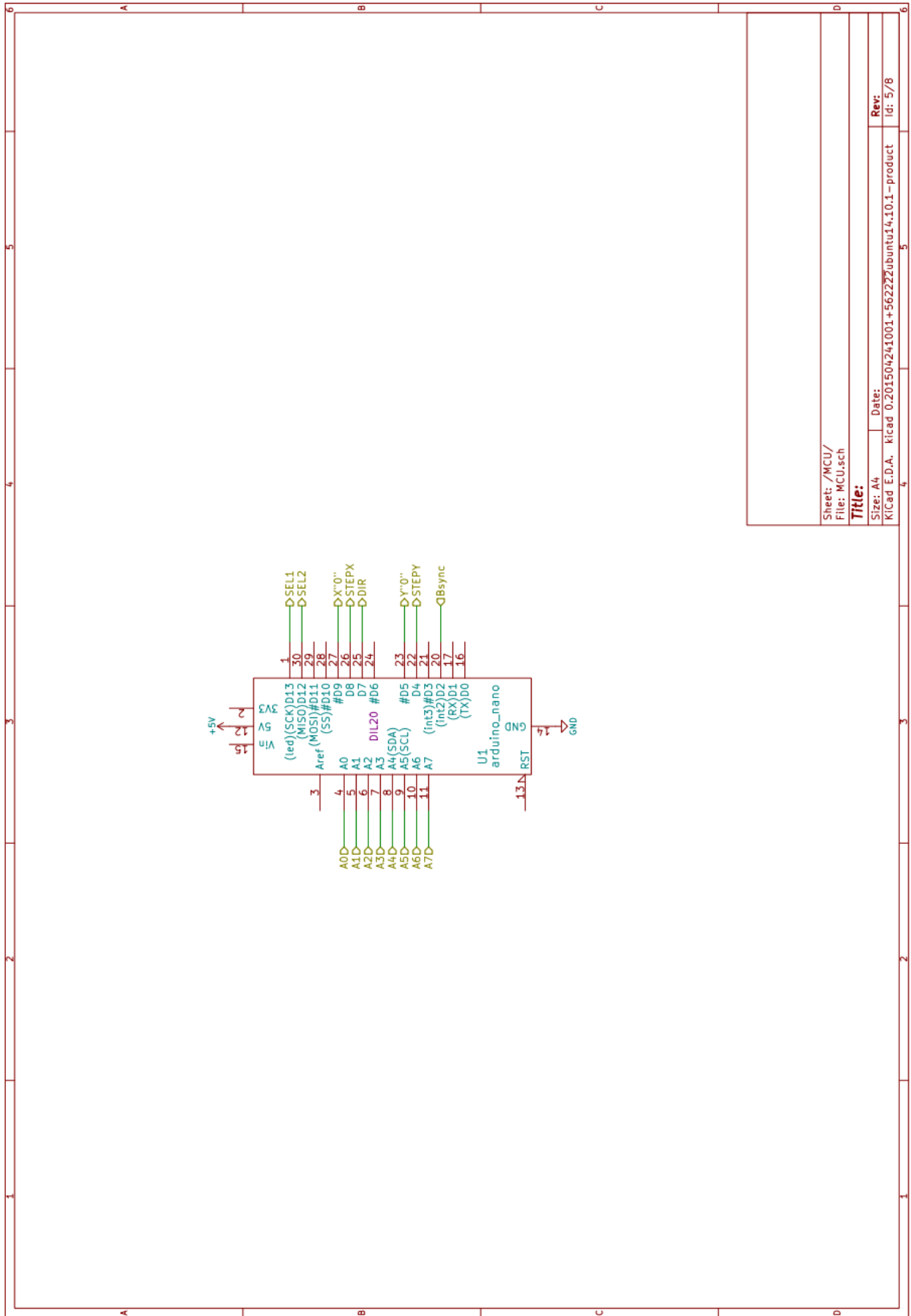
Sheet: /
 File: profilomiter.sch
Title:
 Size: A4
 Date:
 KICad E.D.A. kicad 0.201504241001+562222ubuntu14.10.1-product
 Id: 1/8
 Rev:



Sheet: /Mot_contr/
File: Mot_contr.sch

Title:

Size: A4 Date: Rev: 6/8
KiCad E.D.A. kicad 0.201504241001+562222ubuntu14.10.1 - product Id: 6/8



Sheet: /MCU/
File: MCU.sch

Title:

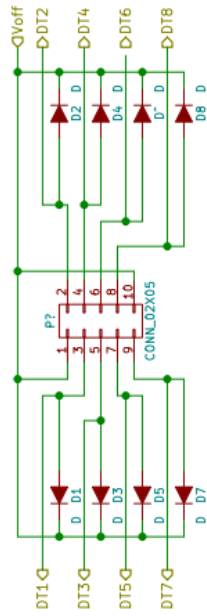
Size: A4

Date:

KiCad E.D.A. Kicad 0.201504241001+56222ubuntutu14.10.1-product

Rev:

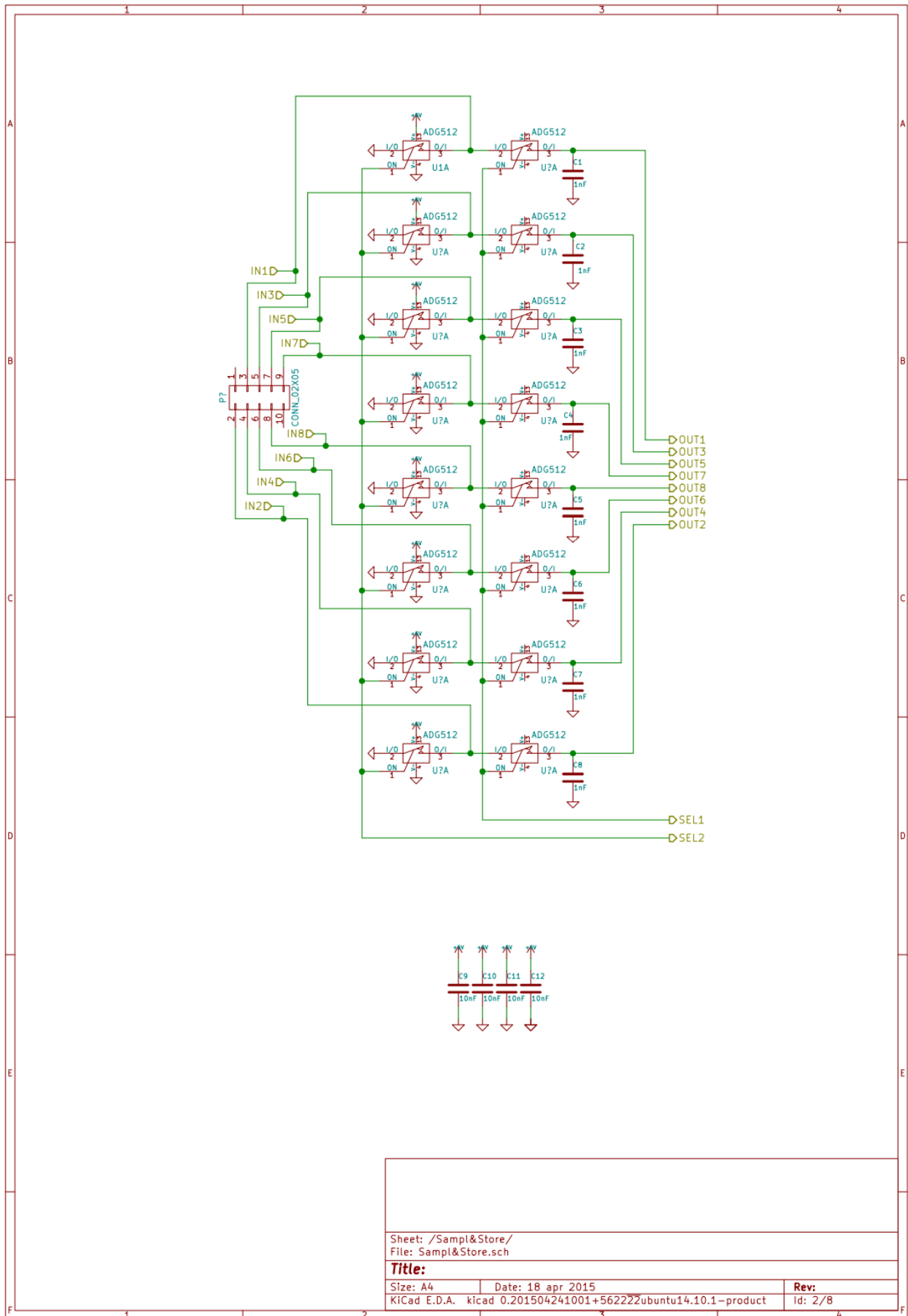
Id: 5/8



Sheet: /detectorX/
 File: detector.sch

Title:

Size: A4 Date: Rev: 3/8
 Kicad E.D.A. Kicad 0.201504241001+562222ubuntu14.10.1-product Id: 3/8



Sheet: /Sampl&Store/ File: Sampl&Store.sch		
Title:		
Size: A4	Date: 18 apr 2015	Rev:
KiCad E.D.A. kicad 0.201504241001+56222ubuntu14.10.1-product		Id: 2/8

Technical task

Ray treatment with proton particles at synchrocyclotron accelerator situated in Saint-Petersburg Nuclear Physics Institute (PNPI) performed using special rotation device (UPST), that helps effectively distribute irradiation dose in determined area of pathological changes of internals, minimizes interaction of irradiation with healthy tissues. Forming of dose field with required configuration caused by coordinated angle adjustment of fixation-device (PF) and medical table (LS) around conjugate focal point where demand dosage building is achieved. Accuracy requirements to the beam forming and leading are quite strict so in spite of using different measurement devices such as profilometers based on proportional wire chambers at the final stage of beam setting examination of its dimensional distribution at the irradiation zone are necessary to be achieved. It can be done using a special semiconducting detector by 2 dimensional scanning of the beam in the plane perpendicular to its distribution. Such device is shown at the photo 1.

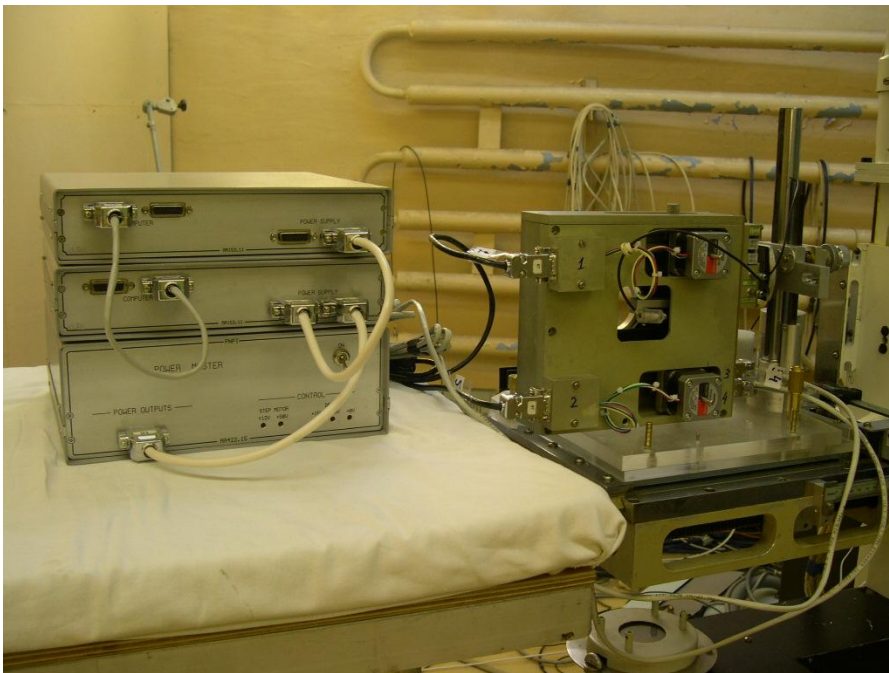


Photo 1.

This device is used at the interpose at the moment is quite heavy and slow. Scanning procedure takes a quite long time. Apparently scanning of the whole area is redundant but changing of the device working algorithm is not possible cause it is too old. Also this device is inharmonious with other used tools and devices, for example with usually used calibration tool shown at the photo 2.



Photo 2.

Was decided to design a small sized scanning device, that can be set directly at calibration tool at three fixed positions (where beam enters the object, escapes the object and in the middle). It is expected to reduce measuring time and simplify the procedure at all by changing its working algorithm, and by removing unnecessary device repositioning and thus its resetting.

Suggested to design a device that consist of two independent mutually orthogonal moving tools with replaceable detection unit.

On the assumption of the fact that device will be used at the final stage of beam forming, when the necessary size of the beam with dimensions proximately 6x6 mm has been already achieved and final setting does not exceeds several unit fraction of millimeter it is rational to limit the measuring tools movements within 18 mm range.

Main technical characteristics expected:

Bounding box: 133mm 20mm 145mm

Analog channels: 8

Maximal movement range: 18mm

Time of full measurement cycle: less than 1-2 mins

Dimension resolution: 0.15mm

Type of the semiconducting detector: Si diode in SOD523 package, SOD123

Supply voltage: +5V

Detection unit has to be done as a separate rapidly replaceable containing from 4 to 8 diode each, depends on the modification.

Director of proton therapy group _____/ D.L.Karlin/